AD NUMBER
AD475018
LIMITATION CHANGES
TO: **Approved for public release; distribution is unlimited.**
FROM: **Distribution authorized to U.S. Gov't. agencies and their contractors; Critical Technology; OCT 1965. Other requests shall be referred to Air Force Materials Laboratory, Wright-Patter son AFB, OH 45433. This document contains export-controlled technical data.**
AUTHORITY
AFML ltr, 22 Aug 1968

SECURITY MARKING

The classified or limited status of this report applies to each page, unless otherwise marked.
Separate page printouts MUST be marked accordingly.

AFML-TR-65-2
Part II, Volume II

TERNARY PHASE EQUILIBRIA IN TRANSITION METAL-BORON-CARBON-SILICON SYSTEMS

Part II. Ternary Systems
Volume II. Ti-Ta-C System

C. E. Brukl
D.P. Harmon
Aerojet-General Corporation

TECHNICAL REPORT NO. AFML-TR-65-2, PART II, VOLUME II
September 1965

Air Force Materials Laboratory
Research and Technology Division
Air Force Systems Command
Wright-Patterson Air Force Base, Ohio

NOTICES

When Government drawings, specifications, or other data are used for any purpose other than in connection with a definitely related Government procurement operation, the United States Government thereby incurs no responsibility nor any obligation, whatsoever, and the fact that the Government may have formulated, furnished, or in any way supplied the said drawings, specifications, or other data, is not to be regarded by implication or otherwise as in any manner licensing the holder or any other person or corporation, or conveying any rights or permission to manufacture, use, or sell any patented invention that may in any way be related thereto.

This report not releasable to (CFSTI) Clearing House for Federal Scientific and Technical Information, formerly (OTS) Office of Technical Services.

Qualified users may obtain copies of this report from the Defense Documentation Center.

The distribution of this report is limited because it contains technology identifiable with items on the Mutual Defense Assistance Control List excluded from export under U. S. Export Control Act of 1949, as implemented by AFR 400-10.

Copies of this report should not be returned to the Research and Technology Division unless return is required by security consideration, contractual obligations, or notice on a specific document.

(18) (19) AFML-TR-65-2- Pt-2-Vol-2

~~Part II, Volume II~~

(6) TERNARY PHASE EQUILIBRIA IN TRANSITION METAL-BORON-CARBON-SILICON SYSTEMS,

Part II. Ternary Systems,
Volume II. Ti-Ta-C System.

(9) Technical rept.,

(10) C. E. Brukl
D. P. Harmon.

(11) Sep 65,

(12) 77p.

(15) AF 33(615)-1249

(16) AF-7350

(17) 735001

007 200

FOREWORD

The work described and illustrated in this report was performed at the Materials Research Laboratory, Aerojet-General Corporation, Sacramento, California under USAF Contract No. AF 33(615)-1249. The contract was initiated under Project No. 7350, Task No. 735001. The work was administered under the direction of the Air Force Materials Laboratory, Research and Technology Division with Captain R. A. Peterson acting as Project Engineer, and Dr. E. Rudy, Aerojet-General Corporation as Principal Investigator. Professor Dr. Hans Nowotny, University of Vienna, Austria, served as consultant to the project.

The project, which includes the experimental and theoretical investigation of selected refractory ternary systems in the system classes Me_1-Me_2-C, Me-B-C, Me_1-Me_2-B, Me-Si-B and Me-Si-C was initiated on 1 January 1964.

The experimental program was laid out by E. Rudy, and the authors wish to acknowledge the many helpful hours given by Dr. E. Rudy to aid in the interpretation of the experimental results. J. Hoffman, R. Radtke, R. Cobb, and J. Pomodoro were of valuable assistance in the preparation of the experimental work. Dr. A. J. Stosick, Senior Scientist, was especially helpful in technically proofreading the manuscript; we are indebted for his helpful criticism.

Chemical analyses of the alloys was carried out under the supervision of Mr. W. E. Trahan, Metals and Plastics Chemical Testing Laboratory of Aerojet-General Corporation. The writers also wish to thank Mr. R. Cristoni, who prepared the many drawings, and Mrs. J. Weidner who typed the report.

The manuscript of this report was released by the authors in August 1965 for publication as an RTD Technical Report.

Other reports issued under USAF Contract AF 33(615)-1249 have included:

Part I. Related Binaries

Volume I. Mo-C System
Volume II. Ti-C and Zr-C Systems

Part II. Ternary Systems

Volume I. Ta-Hf-C System

Part III. Special Experimental Techniques

Volume I. High Temperature Differential Thermal Analysis

Part IV. Thermochemical Calculations

Volume I. Thermodynamic Properties of Group IV, V, and VI Binary Transition Metal Carbides

This technical report has been reviewed and is approved.

W.G. RAMKE
Chief, Ceramics and Graphite Branch
Materials and Ceramics Division
Air Force Materials Laboratory

ABSTRACT

The ternary titanium-tantalum-carbon system was investigated using X-ray, DTA, melting point, and metallographic techniques on chemically analyzed alloys; a complete phase diagram for temperatures above 1500°C was established.

The system contains a rather high melting, continuous monocarbide solid solution with a large carbon defect; a moderate titanium-tantalum exchange occurs in both the high and low temperature modifications of the subcarbide, Ta_2C.

Two four-phase reaction planes are present in the metal-rich portion of the ternary diagram.

The results of this investigation are described, discussed, and compared with another partial investigation of this system; possible applications are briefly mentioned.

TABLE OF CONTENTS

ILLUSTRATIONS

Illustrations (Continued)

Illustrations (Continued)

TABLES

I. INTRODUCTION AND SUMMARY

A. INTRODUCTION

The ternary Ti-Ta-C system has received very little attention during the recent years which have seen so many investigations on carbide binary and ternary systems. This is due,in part,to the fact that titanium is the lowest melting of the refractory metals; detailed information concerning this system was not particularly necessary for the manufacture of cutting tools, some of which are based on mixtures of WC-TiC-TaC, because the metals commonly used as binders are those of the iron group.

Not only would a detailed investigation of the Ti-Ta-C system suggest new application possibilities for composite materials, but far more important, accurately known phase equilibria relationships at high temperatures enable badly needed thermodynamic values to be obtained. These values, when obtained, used in conjunction with data available from the investigations of other carbide systems, provide valuable tools for the prediction of alloy application and behavior in ternary and higher order carbide systems.

The investigations, therefore, were directed toward the establishment of high temperature phase equilibria, determination of the maximum solidus regions, and in particular, the phase relationships in the metal-rich portion of the ternary system. In the majority of instances, graphical presentation of data was given preference over tabular compilation.

B. SUMMARY

The Ti-Ta-C ternary system was investigated using both hot pressed and cold pressed samples. Studies were made using X-ray analysis, differential thermal analysis, metallographic analysis, and

melting point techniques. Many of the alloys prepared were analyzed for their carbon content to check for any possible losses incurred during the various treatments.

1. Binary Systems

The binary tantalum-carbon and titanium-carbon systems have been extensively investigated and recently described in previous reports[1,2] (Figures 1 and 2). The melting behavior of titanium-tantalum alloys was studied, and a constitution diagram (Figure 6) of the Ti-Ta system in the solidus-liquidus region developed. The complete solid solution shows two phase melting; the results are in good agreement with those presented in Hansen's Constitution of Binary Alloys[35]

2. Ternary Titanium-Tantalum-Carbon System (Figure 45)

a. Monocarbide Region

The face centered cubic binary phases, $TaC_{0.94}$ ($a = 4.456$ Å) and $TiC_{0.94}$ ($a = 4.330$ Å), form a continuous series of solid solutions; the lattice parameters show an almost linear dependence on the metal concentration, (Figure 10). The melting points of the monocarbide solid solution decrease from TaC_{1-x} to TiC_{1-x} (Figure 41).

b. Carbon-Rich Equilibria

There are no other ternary phases except the monocarbide solid solution in this area. The monocarbide-carbon eutectic trough runs almost linearly across this region (Figure 48) between the Ta-C binary eutectic at 61 At% C and the Ti-C eutectic at 63 At% C; the eutectic temperatures decrease smoothly from 3445°C on the tantalum side to 2776°C on the titanium side (Figure 42).

c. Metal-Rich Equilibria

Two four-phase reaction planes are present in the region between the monocarbide solid solution and the metal phase.

(1) Class II Four-Phase Equilibrium at 2020°C (II_a in Figure 48)(Figure 54)

The four-phase reaction occurring at this temperature is represented by the following reaction equation:

$$\text{Liquid} + \beta\text{-(Ta, Ti)}_2\text{C}\ (\gamma') \underset{T \geq 2020°C}{\overset{T \leq 2020°C}{\rightleftharpoons}} \text{(Ti, Ta)C}_{1-x}\ (\delta) + \text{(Ti, Ta)}(\beta)$$

Table 1: Four-Phase Reaction Plane

$\text{Liq.} + \gamma' \rightleftharpoons \delta + \beta$ at 2020°C

Equilibrium Concentrations of Partaking Phases

Phase	Concentrations in At% Ti	Ta	C
Liquid	47	49	4
$(Ta, Ti)_2C(\gamma')$	32	36	32
$(Ti, Ta)C_{1-x}(\delta)$	48	16	36
(Ti, Ta) (β)	40	59	~ 1

(2) Class I Four-Phase Equilibrium at 1815°C (I_b in Figure 28) (Figures 37 and 51)

The four-phase reaction occurring at 1815°C can be represented by the following reaction equation:

$$\beta\text{-(Ta, Ti)}_2\text{C}\ (\gamma') \underset{T \geq 1815°C}{\overset{T \leq 1815°C}{\rightleftharpoons}} \alpha\text{-(Ta, Ti)}_2\text{C}\ (\gamma) + \text{(Ti, Ta)C}_{1-x}\ (\delta) + \text{(Ti, Ta)}(\beta)$$

Table 2: Four-Phase Reaction Plane

$\gamma' \rightleftharpoons \gamma + \delta + \beta$ at 1815°C

Equilibrium Concentrations of the Partaking Phases

Phase	Concentration in At% Ti	Ta	C
β-$(Ta, Ti)_2C(\gamma')$	~31	37	32
α-$(Ta, Ti)_2C(\gamma)$	~29	39	32
$(Ti, Ta)C_{1-x}(\delta)$	48	17	35
(Ta, Ti) (β)	35	64	~1

At temperatures below the 1815°C four-phase reaction plane, only the low temperature α-form of the subcarbide is present; the maximum "Ti_2C" solubility in α-Ta_2C at the 1815°C four-phase plane is approximately 43 mol.%. The β-form of $(Ta, Ti)_2C$ takes about 47 Mol.% "Ti_2C" into solution at 2020°C, the temperature of the second four-phase plane.

In the extreme metal-rich portion of the ternary diagram, a ternary eutectic trough connects the titanium-carbon binary eutectic at approximately 1.5 At.% carbon with the tantalum-carbon eutectic at 12 At.% carbon (Figures 27 and 48). The melting points of the eutectic trough rise along a smooth curve from the Ti-C binary at 1650°C to 2843°C at the Ta-C binary.

II. LITERATURE REVIEW

A. BINARY SYSTEMS

The titanium-carbon system has been the object of numerous investigations[4-9]. A listing of the many papers is found in Constitution of Binary Alloys[3].

The main features of the system, taken from the older literature, are as follows: There exists but one compound, the monocarbide, with an extensive homogeneous range and melting point in excess of 3000°C. The β-Ti decomposes peritectically at approximately 3 At% C, and the

peritectic or eutectic temperature with TiC_{1-x} is 1750°C. The solubility of carbon in β-titanium increases to a maximum of about 3 At% at the proposed peritectic temperature. The α-β-titanium transition is extended peritectoidally into the binary at 920°C. The eutectic between the monocarbide and graphite lies at about 63 At% C at a temperature of approximately 2900°C. A recently proposed constitution diagram of the Ti-TiC system[10] by E. K. Storms agrees quite well with the experimental results described below.

To clarify the discrepancies in the binary Ti-C system, and to provide valid starting points for the ternary systems to be studied in this present series of investigations, an exact determination of the constitution of the titanium-carbon system was undertaken at this laboratory[1]. The important features of the system at temperatures above 1200°C are: (Figure 1) titanium monocarbide possesses a wide homogeneous range from 32 At% C at the eutectic temperature of 1650°C to 48.8 At% C; it melts congruently at 3067°C at 44 At% C. Between β-titanium, whose carbon solubility is less than 1 At%, and the carbon-defect monocarbide there is a eutectic at 1.5 At% C. The eutectic temperature is 1650°C. On the carbon-rich side of the monocarbide a eutectic exists at 63 At% C between $TiC_{0.94}$ and graphite. The eutectic temperature is 2776°C. The maximum lattice parameter of the cubic monocarbide structure is 4.330 Å at 48.5 At% C; the smallest is 4.285 Å on the metal-rich boundary (32 At% C) of the homogeneous range.

Literature reveals that there are a great number of publications[11-22] concerning the tantalum-carbon system; although many corrections and additions had been made in recent years, the basic diagram

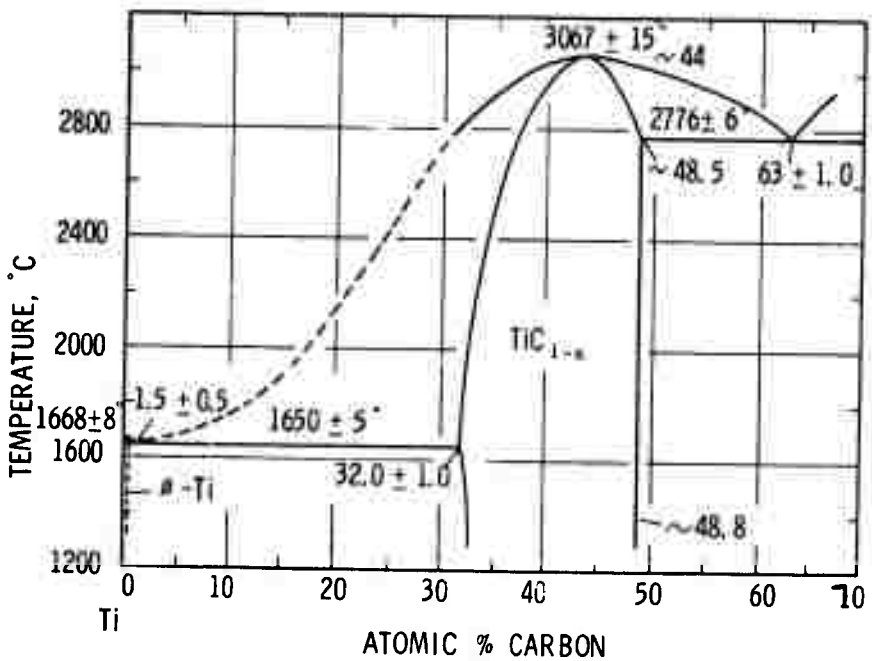

Figure 1. Ti-C: Constitution Diagram
(E. Rudy, C. E. Brukl, and D. P. Harmon, 1965)

established by F. H. Ellinger[16] had remained. Its main features are two compounds, Ta_2C and TaC; both compounds have considerable homogeneous ranges. Tantalum subcarbide decomposes peritectically at 3400°C, and TaC melts congruently at about 3800°C. Tantalum monocarbide and graphite form a eutectic at about 66 At% C with a eutectic temperature of 3300°C. Between the subcarbide, Ta_2C, and the tantalum metal solid solution, there exists a eutectic at about 5 At% C; the eutectic temperature is 2800°C. At this temperature, the carbon solubility in the tantalum metal phase is approximately 3 At% C.

Within the framework of these present investigations the tantalum-carbon system has been most thoroughly investigated[2] by X-ray analyses, melting point determinations, metallography, and differential thermal analysis.

An α-β-transformation — a fact which had been reported[18] but not confirmed[12, 16, 22] — involving the degree of ordering of the carbon atoms in the carbon sublattice in Ta_2C, was irrevocably established. The presence of a "Ta_3C_2" metastable phase, reported by G. Brauer[17] was observed, but attributed to a non-equilibrium phase resulting from precipitation from the monocarbide phase.[2, 12]

The main points of the tantalum-carbon system are shown in Figure 2. Tantalum metal takes about 7.5 At% C into solid solution at 2843°C. Between tantalum metal and the high temperature form of Ta_2C (β) there is a eutectic at 12 At% C; the eutectic temperature is 2843°C. The β-Ta_2C has a homogeneous range from 26 At% C at 2843°C to about 35.5 At% C at 3300°C; it decomposes eutectoidally into the low temperature Ta_2C (α) and TaC_{1-x} at 1930°C at low temperatures, and decomposes peritectically at 3330°C at high temperatures. α-Ta_2C, which has a small homogeneous range around 31 At% C, decomposes in a peritectoid reaction to tantalum metal and β-Ta_2C at 2180°C.

The monocarbide shows a homogeneous range of a carbon defect solid solution from 49.8 At% C to about 39 At% C at 3330°C; $TaC_{0.89}$ melts congruently at 3983°C. The eutectic formed between the monocarbide and graphite lies at 61 At% C; this eutectic temperature is 3445°C.

All investigations of the tantalum-titanium system[23-27] agree in general. Tantalum and β-titanium form a continuous series of

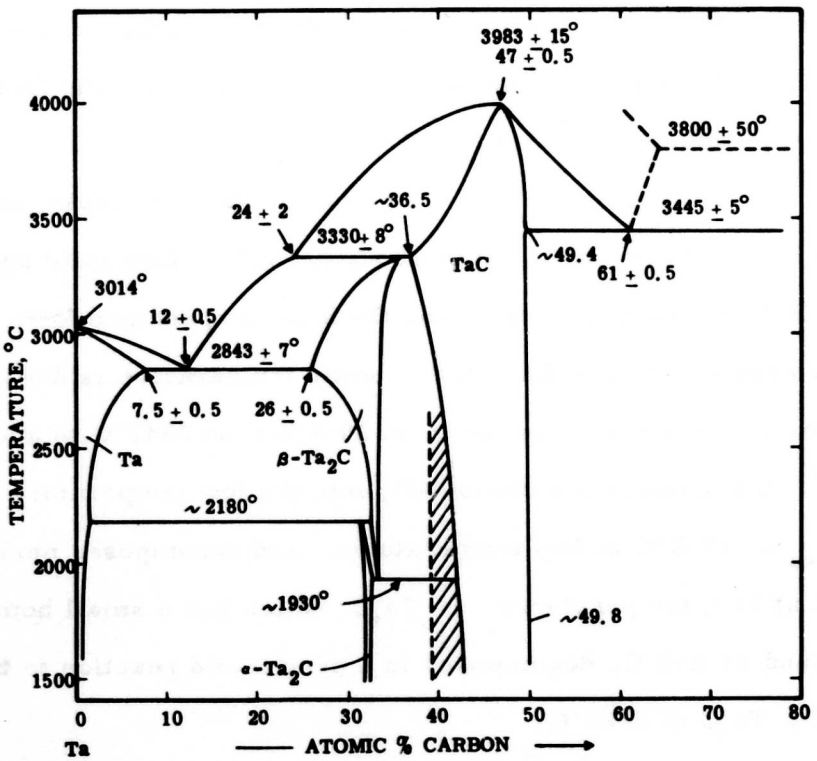

Figure 2. Ta-C: Constitution Diagram
(E. Rudy, C. E. Brukl, and D.P. Harmon, 1965)

solid solutions above the α-β-transition temperature of titanium (~920°C). The solubility of tantalum in α-titanium appears to be quite small (~4 At%), and the α-β-titanium transition temperature is decreased with increasing tantalum content. A composite picture (Figure 3), containing data from D. Summers-Smith[25] on one hand, and D. J. Maykuth, et.al.[26] on the other, shows the liquidus- solidus high temperature region of the tantalum-titanium system.

B. TERNARY TITANIUM-TANTALUM-CARBON SYSTEM

The quasi binary section TaC-TiC had been investigated as early as 1946-47. Nowotny and Kieffer[29], as well as Koval'skii and Umanskii[30] had ascertained that TaC and TiC form a continuous series of solid solutions. These investigations were later confirmed by other authors[31, 33](Figures 4 and 5).

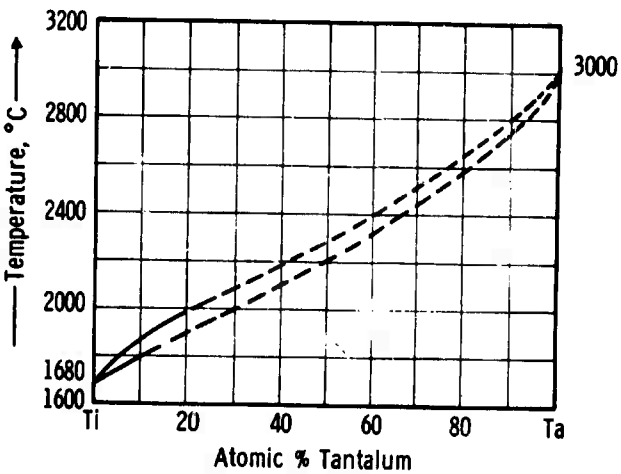

Figure 3. Ti-Ta: Composite Constitution Diagram of High Temperature Region
(D. Summers-Smith; and D.J. Maykuth, et.al. as cited in M. Hansen[28])

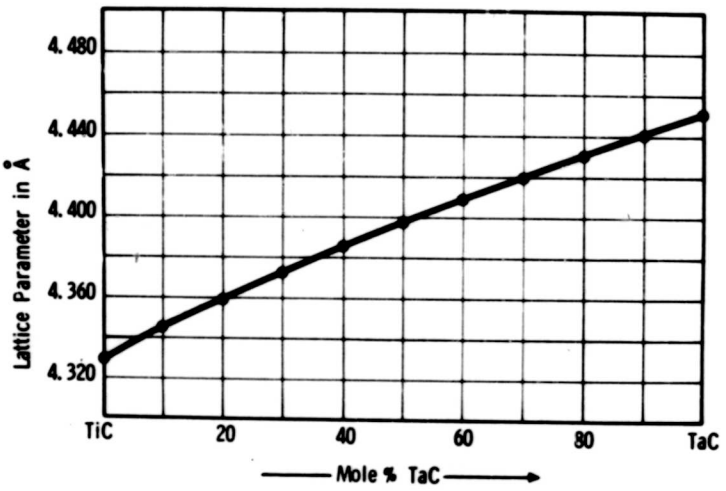

Figure 4. Ti-Ta-C: Lattice Parameters of TaC-TiC Solid Solution (J.G. McMullin and J. T. Norton, 1953)

J. G. McMullin and J.T. Norton[31] presented an isothermal section of the Ti-Ta-C system at 1820°C (Figure 5). In investigations up

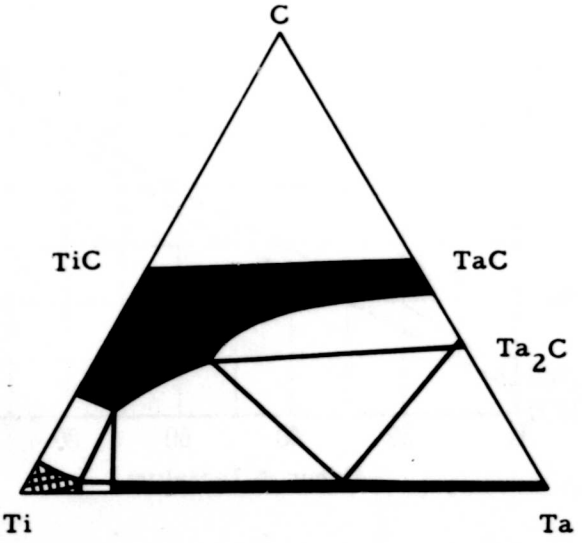

Figure 5. Ti-Ta-C: Isothermal Section at 1820°C (J. G. McMullin and J. T. Norton, 1953)

to about 2030°C, it was shown that titanium and tantalum form a continuous series of solid solutions above the α-β-transition of titanium; this solid solution can take up to 2 At% carbon into solution. The monocarbides form a rather large single-phase area showing a large carbon defect, mixed crystal solid solution on the titanium side. Conversely, the Ta_2C subcarbide phase is shown to dissolve none of its hypothetical homologue "Ti_2C". A three-phase region $(Ti, Ta)C_{1-x}$ — $(Ta, Ti)_2C$ — (Ti, Ta) exists in the middle and tantalum-rich portion of the 1820°C isothermal section; the equilibrium in the titanium-rich corner of the system is governed by liquid at 1820°C. These authors have further determined that the basic equilibrium described above remains up to 2025°C where a four-phase invariant reaction plane is situated. The so-called "two over two", or a simple Class II_a* reaction occurs at this temperature. The two-phase equilibrium $(Ti, Ta)C_{1-x}(\delta)$ - (Ta, Ti)(β) is replaced by the $(Ta, Ti)_2C$ (γ)-Liquid (Ti-rich) equilibrium and is formulated by the following reaction:

$$Liq + \gamma \rightleftarrows \delta + \beta \qquad \text{at } 2025\,^{\circ}C$$

III. EXPERIMENTAL PROGRAM

A. EXPERIMENTAL PROCEDURES

1. Starting Materials

Elemental powders as well as pre-prepared binary monocarbide and titanium hydride powders were used as starting materials for the alloys investigated.

---

*The excellent book, Phase Diagrams in Metallurgy, by F. Rhines was extensively consulted in regard to nomenclature and equilibria questions. The nomenclature proposed therein has been used in this report.

Titanium metal powder was obtained from the Var-Lac-Oid Chemical Company, New York, and had the following impurities (in ppm): C-1300, H-1500, N-50, Fe-500 and Cl-1200. The lattice parameters of this starting material, as determined with CuK_α, were a = 2.94$_9$ Å and c = 4.68$_8$ Å. The particle size was smaller than 74 microns.

Titanium dihydride, Grade E, purchased from Metal Hydrides, Inc., Beverly Mass., had the following impurities (in ppm): Al-1000-3000, C-1000 max., Ca-500 max., Fe-1000 max., Mg-500 max., N-2000 max., Si-1000 max., and Zr-1000 max.; the hydrogen content was 3.99% by weight. This titanium hydride had an average particle size of 7.3 microns. A Debye-Scherrer powder diagram of this material showed only the face centered cubic dihydride structure. Spectrographic analysis at the Aerojet Metals and Plastics Chemical Testing Laboratory resulted in the following data (in ppm): Cr-400, Al-10, Fe-100, Zr-50, and Ca-100.

Tantalum monocarbide was obtained from Kennametal, Inc., Latrobe, Pennsylvania. The impurities were (in ppm): Nb-1500, Fe-200, Si-100, Ti-< 100 and Ca-100. The tantalum carbide contained 6.17 Wt% total carbon (49.8 At%) and 6.11 Wt% bound carbon (49.5 At%). The particle size was smaller than 44 microns. 4.455 Å was obtained as the lattice parameter of this starting material.

Var-Lac-Oid, Inc., New York supplied the titanium monocarbide powder. The impurities were (in ppm): Fe-500, Si-100, Ca-100, Na-50, O-1000, and N-1500. The monocarbide had a total carbon content of 19.50 Wt% C (49.1 At%) and 19.30 Wt% bound carbon (48.8 At%). The lattice parameter of this starting material was 4.323 Å, and the particle size was smaller than 88 microns.

Carbon was used in two forms. The lampblack powder, supplied by Monsanto Chemical Co., had 99.57% free carbon and the following impurities (in ppm): H_2O-400, benzol extract-3000, ash-300, and volatiles-3600. The particle size was 0.01-0.1 microns. Spectrographic analysis at the Aerojet Metals and Plastics Chemical Testing Laboratory gave the following results (in ppm): Si-20, Mg-< 10, Cu-< 10, Al-10, Fe-10.

Graphite powder was obtained from the National Carbon Company and had the following typical impurities (in ppm): S-110, Si-46, Ca-44, Fe-40, Al-8, Ti-4, Mg-2, V-trace, and ash-800 max. 99% of the graphite was smaller than 74 microns. Highly overexposed X-ray films of these materials showed no traces of any impurities.

Tantalum metal powder was obtained from the Wah Chang Corp., Albany, Oregon. The powder, which had a particle size smaller than 74 microns, had the following main impurities (in ppm): Al-< 20, C-73, Cu-< 40, Cr-< 20, Fe-275, H-21, N-5, O-238, Si-<100, Ti-< 150, W-220, and Nb-630. The lattice parameter of this starting material was 3.303 Å.

A vacuum fusion analysis performed at the Aerojet Metals and Plastics Chemical Testing Laboratory yielded the following data for the tantalum powder (in ppm): H-116, O-322, and N-52. Spectrographic analysis gave (in ppm): C-180, Si-< 20, Fe-500, Nb-2500, and Al-< 20.

2. Alloy Preparation and Heat Treatment

In the ternary system Ti-Ta-C, all alloys for solid state and melting point investigations, as well as for arc melted samples, were initially prepared by hot pressing in graphite dies. The samples for solid state investigations were heat treated at two principal temperatures,

1500 and 2000°C, under a vacuum of $< 5 \times 10^{-5}$ Torr. These samples were quenched rapidly by immediately admitting helium to the vacuum chamber after shutting off the heating element of the furnace. A detailed heat treating schedule is given in Table 3.

Table 3: Heat Treatment Schedule of Titanium-Tantalum-Carbon Alloys

Equilibrium Temperature °C.	Annealing Time (Hrs)	Vacuum
1500	40-64	$< 3 \times 10^{-5}$ Torr
2000	4-21	5×10^{-5} Torr

For solid-state investigations approximately 0.1-0.5 Wt% cobalt powder, which later completely disappears during the vacuum heat treatment, was added to the samples in the high melting monocarbide region to aid in the attainment of equilibrium. In general, the alloys were found to have attained equilibrium in the majority of samples investigated. Only those samples which were situated in the tantalum subcarbide region showed somewhat diffuse diffraction patterns caused by the α-β-Ta_2C transformation. Small amounts of the β-phase, normally not present at 1500°C, formed at higher hot pressing temperatures and did not completely transform to the low temperature α-phase during heat treatment at 1500°C. Various stages of non-equilibrium, dependent on the amount of tantalum present, were also obtained in the titanium-rich corner of the ternary where the high temperature β - Ti - form was not completely retained on cooling.

Powdered mixtures of the elements, to serve as melting point specimens in the Ti-Ta binary system, were cold-compacted to avoid graphite contamination. The samples received a heat treatment at

1350°C under a vacuum of 5×10^{-5} Torr for 1 hour to give the melting point specimens mechanical strength and to cause partial mixed crystal formation.

Portions of some samples (Figure 15) which were used in the solid state studies were arc melted in a non-consumable tungsten electrode melting furnace. These samples were then X-rayed and investigated metallographically along with the molten portions of the melting point samples.

3. Melting Points

The melting points of alloys selected were determined by the previously described Pirani-technique[33]. To minimize the titanium and carbon losses at the high melting temperatures of the monocarbide region, the melting point furnace was pressurized with high purity helium at 2 1/4 atmospheres after a short vacuum degassing at about 2200°C. The temperature measurements were carried out with a disappearing-filament type micropyrometer which was calibrated against a certified, standard lamp from the National Bureau of Standards. The temperature correction for absorbtion in the quartz furnace window, as well as that correction for deviation due to non-black body conditions, have been amply described and validated in a previous report[33].

Fifty-seven individual alloy compositions (Figure 14) were made and their melting points measured. All of these samples were further investigated by studying their X-ray diffraction patterns; the majority of these melting point samples were mounted and observed metallographically; several samples were analyzed for their total carbon content. In no case did the analyzed values of carbon content differ by more than 1-2 At% from the nominal compositions.

4. Differential Thermal Analysis

The techniques, equipment, and instrumentation used for high temperature differential thermal analysis have been described at length in previous publications[33, 34].

The 13 DTA samples (Figure 16) investigated in this system were prepared by hot pressing the well blended mixtures of elemental powders and the monocarbides. Investigations were made under a protective high-purity helium atmosphere at 2 atms.pressure. The DTA technique proved exceptionally valuable in determining the temperature-composition paths of the phase reactions present in the binary systems and continuing or terminating in the ternary Ti-Ta-C system. In addition, the DTA served to confirm incipient melting temperatures of the solidus boundaries close to homogeneous ranges; these temperatures are usually difficult to observe using the Pirani-method because relatively little liquid is present at the incipient melting temperature. This technique was instrumental in helping to ascertain the temperatures of the four-phase reaction planes occurring in the ternary system. The incipient melting point of alloys in the four-phase quadrant was best obtained with the DTA rather than the Pirani melting point method, for the same reasons as described above.

5. Metallography

Thirty-three samples, which had been either arc melted, or melted in the melting point, or DTA furnaces were metallographically examined. The specimens were mounted in an electrically conductive mixture of diallylphtalate-lucite-copper mounting material. Coarse grinding and rough polishing were done on varying grit sizes

(120-600) of silicon carbide paper. A fine, highly polished sample surface was ultimately obtained using a suspension of 0.05 micron alumina in Murakami's solution on microcloth. Etching solutions and techniques varied greatly with the carbon content of the ternary alloys. It was found that samples in the metal-rich region up to about 15 At% carbon were best electroetched with a 2% NaOH solution. Alloys containing higher amounts of carbon gave best results when dip-etched in an aqueous-aqua regia-hydrofluoric acid mixture, (9 parts H_2O with 1 part of a 60% HCl -20% HNO_3-20% HF concentrated acid solution). A concentrated solution of the above acid mixture was used to bring out the grain boundaries of single phase monocarbide alloys.

6. X-Ray Analysis

Debye-Scherrer powder diffraction patterns, using CuK_α radiation, were made of all samples after solid state, melting point, and DTA investigations, as well as of arc melted samples.

To eliminate the film-blackening caused by titanium flourescence radiation, induced by the CuK_α, a cover film, which absorbed this soft white radiation was used over the film during the exposure.

The crystal structures of all the binary phases with the exception of the "Ta_3C_2" zeta phase are known, and the indexing of the powder patterns, as well as lattice parameter determinations offered no problems.

Some difficulties, however, were encountered in the metal-rich portion of the ternary system where the α-β-titanium transformation occurred, causing broad lines and diffuse patterns. In addition to this, the fact that the body-centered-cubic lattice parameters of tantalum

and β-titanium show very little difference made precise concentration determinations difficult.

7. Chemical Analysis

Carbon analyses were performed using the standard direct combustion method, and either trapping the evolved CO_2 on NaOH and computing carbon content by weight gained, or by measuring the thermal conductivity of the combusted CO_2-O_2 gas mixture in a Leco carbon analyzer.

The oxygen, nitrogen, and hydrogen analyses were carried out using the vacuum fusion technique in a platinum bath. In general, the interstitial contents reported by the Aerojet Metals and Plastics Chemical Testing Laboratory tended to be somewhat (~10%) higher than those values reported by the producer. This discrepancy is perhaps explained by the fact that the materials, in their fine powder form, had sufficient time to absorb both additional water vapor and air in the time interval between the supplier's analysis and the Quality Control analysis at Aerojet.

Far more important, however, were the spectrographic analyses performed in a semiquantitative manner to check on the metallic impurities. Excessive amounts of these impurities could easily lead to false phase equilibria and homogeneous ranges in the investigated Ti-Ta-C system. Furthermore, metallic impurities, if present in excessive quantities, would critically change the melting points of the investigated alloys. The spectrographic analyses showed no great contamination of any one particular element, and in general, the overall sum of metallic impurities was reasonably low and well within tolerable limits.

B. EXPERIMENTAL RESULTS

1. Titanium-Tantalum Solidus

The melting points of seven samples of the nominal compositions shown in Figure 6 were measured. The solidus line is a well defined, smooth curve; with increasing tantalum content, the alloys were observed to melt more and more heterogeneously. This fact is reflected in the increasing width of the two-phase liquid-solid region bounded on the liquidus side by the estimated liquidus line. The melting points of the pure metals are those which were very accurately obtained in other investigations[1,2] in this laboratory. The diagram proposed here agrees quite well with those in the literature[35] (Figure 3) with the exception that the liquid-solid two-phase region is somewhat wider.

2. Titanium-Tantalum-Carbon System

Forty-nine ternary alloys were prepared to investigate the solid state section at 1500°C; the compositional locations are shown in Figure 7.

Figure 8 depicts the qualitative X-ray analysis and phase equilibria of the samples at 1500°C. At 1500°C, titanium and tantalum form a complete series of solid solutions in the body-centered-cubic structure. Due to the relatively small change in lattice parameter of the binary b.c.c. solid solution (Ta = 3.30 Å and β-Ti = 3.31 Å), it was virtually impossible to determine the metal-rich base point of the (Ta, Ti)-α-$(Ta, Ti)_2C$-$(Ti, Ta)C_{1-x}$ three-phase region by a comparison of metal phase lattice parameters taken from samples in this three-phase area. More value, therefore, had to be placed on the qualitative X-ray analysis of the samples. The base point of the three-phase (Ta, Ti)-α-$(Ta, Ti)_2C$-$(Ti, Ta)C_{1-x}$ region was located quite close to 32 At% Ti using the method of appearance and disappearance of phases.

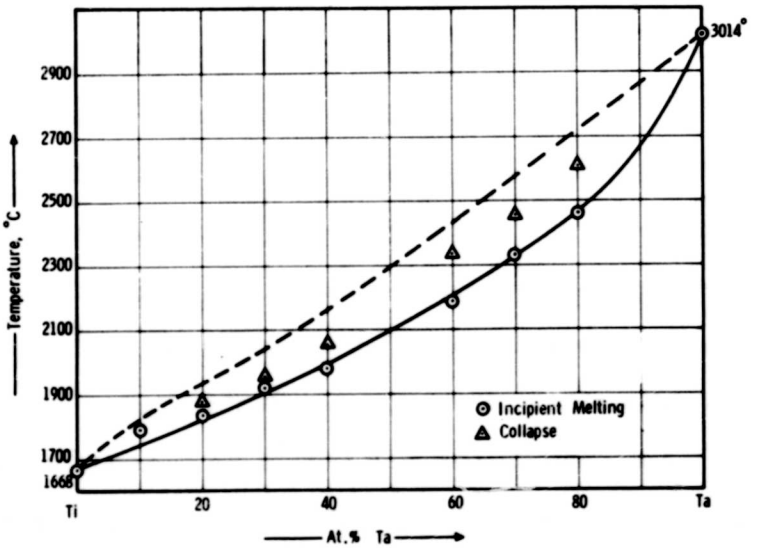

Figure 6. Ti-Ta: Constitution-Diagram, Liquid-Solid Region with Experimental Melting Points.

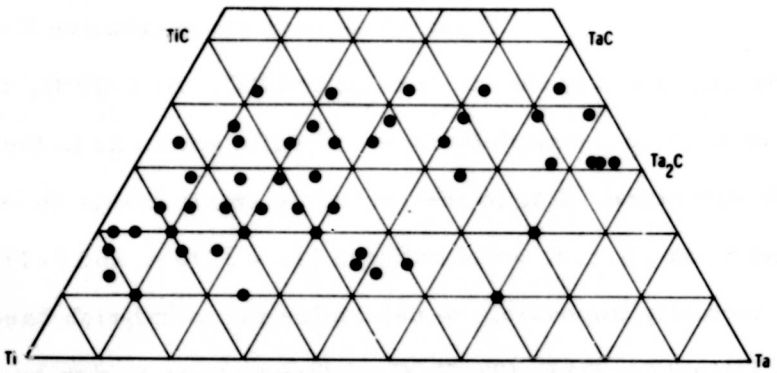

Figure 7. Ti-Ta-C: Location of Solid State Samples at 1500°C

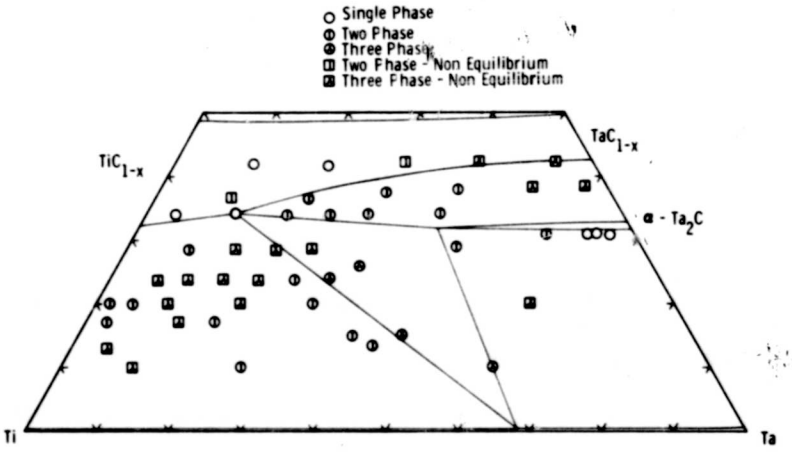

Figure 8. Ti-Ta-C: Qualitative X-ray Analysis of Samples at 1500°C

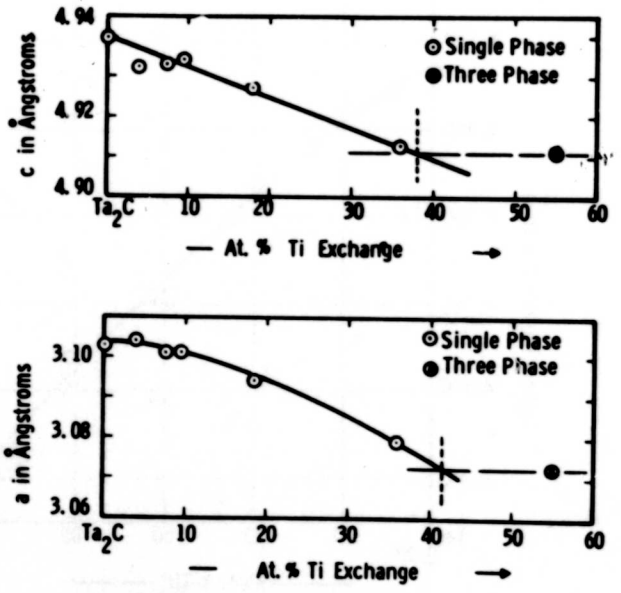

Figure 9. Ti-Ta-C: Lattice Parameters of α-$(Ta, Ti)_2C$ at 1500°C

At 1500°C only the low temperature α-form of Ta_2C is present. A plot of lattice parameters vs composition (Figure 9) shows that α-Ta_2C takes about 40 mol % "Ti_2C: into solid solution; the smallest lattice constants, taken from a sample in the three-phase region, were found to be a = 3.07_1 Å, c = 4.91_1 Å.

The tantalum and titanium monocarbides form a complete series of solid solutions with a considerable carbon defect which increases with increasing titanium content. The lattice parameters of the face-centered-cubic mixed crystal plotted versus titanium content (Figure 10) confirm the presence of the continuous solid solution; a slight

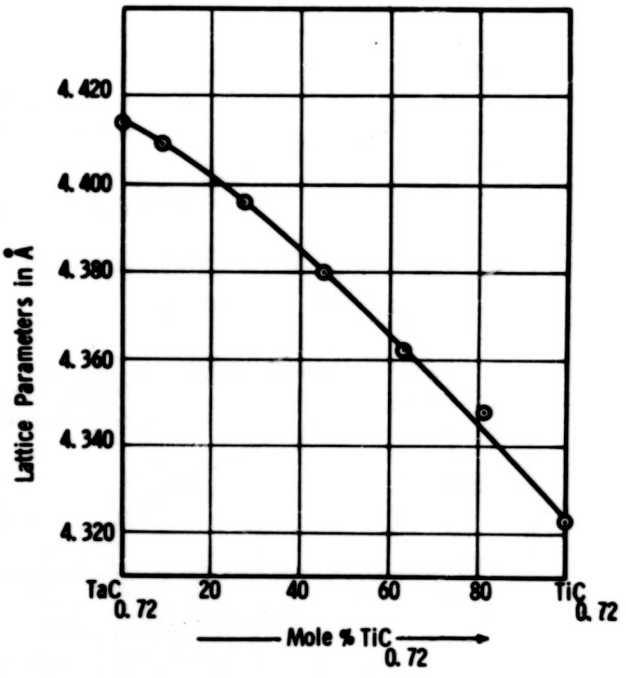

Figure 10. Ti-Ta-C: Lattice Parameters of (Ta, Ti)$C_{0.72}$ Monocarbide Solid Solution at 1500°C

positive deviation from Vegard's law is noted. The three-phase area base point which rests on the lower boundary of the monocarbide region was found to be at 34 At% carbon and 12 At% tantalum.

The X-ray powder diagrams of some of the samples near the Ta-C binary, and extending into the ternary, showed the presence of the metastable zeta "Ta_3C_2" phase in varying amounts; in view of the results of the binary Ta-C system[2], it was concluded that this phase is precipitated from the metal-rich region of the monocarbide single phase and actually represents a non-equilibrium state. The X-ray analysis (Figure 8) indicates this conclusion, and phase equilibria which would be present due to the zeta phase are not depicted. Figure 49 shows the 1500°C isotherm.

The two-phase (Ti, Ta)C_{1-x}-(Ti, Ta) region exhibits a number of non-equilibrium samples. This is simply explained by the fact that the high temperature β-(Ti, Ta) cubic form transforms quite rapidly, but not completely, to the α-(Ti, Ta) hexagonal structure. Increasing amounts of tantalum shift this transformation to lower temperatures, and the β-form is more completely retained.

In a very few samples, in the vicinity of the subcarbide, it was occasionally found that traces of TaC_{1-x} were present after heat treatment. The presence of the monocarbide represents a non-equilibrium condition and is most probably caused by the disproportionation of the subcarbide solid solution upon cooling. In addition, traces of the starting material, TaC, might still have been present after heat treatment. Such was the case with the sample in the two-phase α-(Ta, Ti)$_2$C-(Ta, Ti) region.

Portions of some of the 1500°C heat treated samples remaining after X-ray and chemical analyses were given a further heat treatment at 2000° (Figure 11).

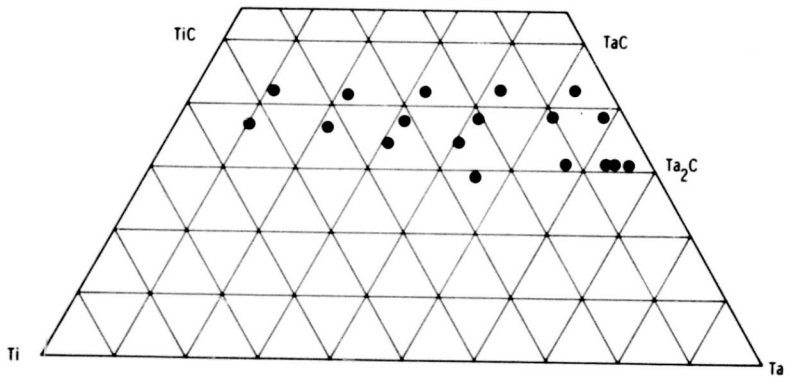

Figure 11. Ti-Ta-C: Location of Solid State Samples at 2000°C

Again, several samples showed the presence of the metastable zeta phase, but that which was previously stated in the 1500°C section description also applies to this 2000°C isotherm. Figure 12 shows the qualitative X-ray analysis of the samples in the still solid region.

The high temperature form, β-Ta_2C, plays a leading role in the phase equilibria at 2000°C. The X-ray patterns of the $(Ta, Ti)_2C$

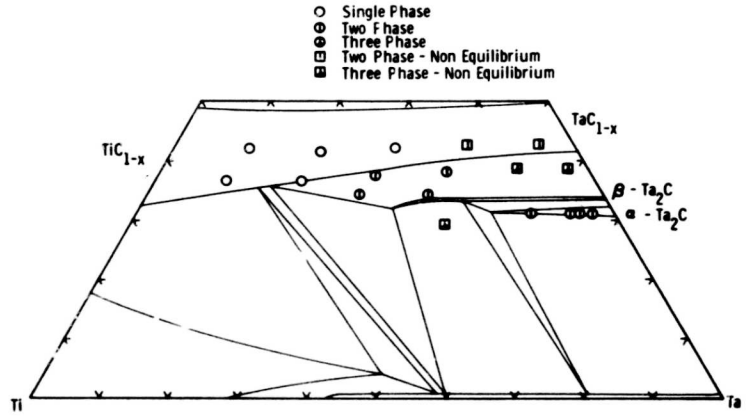

Figure 12. Ti-Ta-C: Qualitative X-Ray Analysis of Samples at 2000°C.

phase were in general less sharp than the corresponding patterns at 1500°C; this is due to the β-α-transformation upon cooling. In addition, precipitations of the metastable zeta phase, as well as the subcarbide phase from the monocarbide solid-solution led to somewhat diffuse X-ray patterns. A photomicrograph of a sample whose X-ray film showed (Ta, Ti)C_{1-x}, ζ, and (Ta, Ti)$_2$C is shown in Figure 13.

The rapid disproportionation of the β-(Ta, Ti)$_2$C to a α-(TaTi)$_2$C less rich in titanium, monocarbide, and metal phase made the exact measurement of the solubility limit of (Ta, Ti)$_2$C rather difficult. However, a comparison of the X-ray films of the 2000°C samples with those of melting point samples, as well as metallographic inspection led to the determination of the maximum tantalum-titanium exchange in β-(Ta, Ti)$_2$C. At 2000°C the exchange is not much more than that of the α-form at 1500°C; the maximum solubility in the β-form is about 46 mol % "Ti_2C".

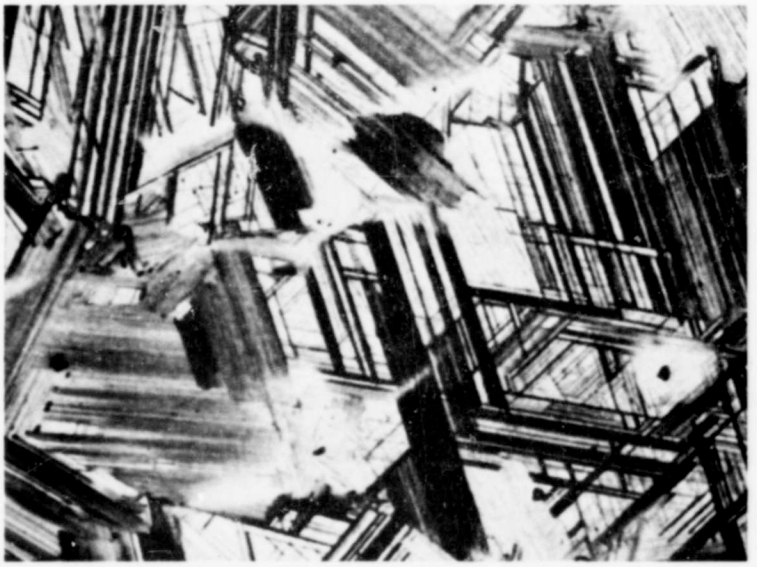

Figure 13. Ti-Ta-C: 17/50/33, Quenched from 3260°C X1000
$(Ta, Ti)C_{1-x}$ Solid Solution with Oriented Precipitations of ζ and $(Ta, Ti)_2C$.

Extensive metallography of melting point, arc melted, and DTA samples (location of samples in Figures 14, 15,and 16) as well as comparison of the ternary melting points with those of the metal binary showed that the metal-rich eutectic trough lies quite close to the Ti-Ta binary across the greater portion of the ternary diagram (Figures 27 and 48). In general, it was quite difficult to obtain pictures typical of a eutectic in this region. The main cause for this is that the eutectic contains a relatively small percentage of the carbide phases. In addition to the above, it was observed that when the carbides were present, they tended to migrate to, and agglomerate on the grain boundaries giving a very non-typical net-like structure. Even the most rapidly cooled alloys showed this effect in varying degrees. A third factor contributing to this difficulty

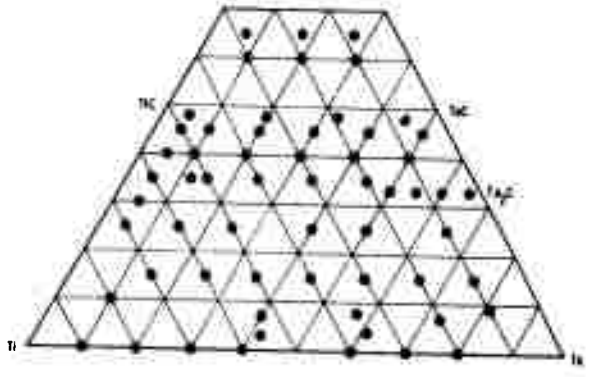

Figure 14. Ti-Ta-C: Location of Melting Point Samples

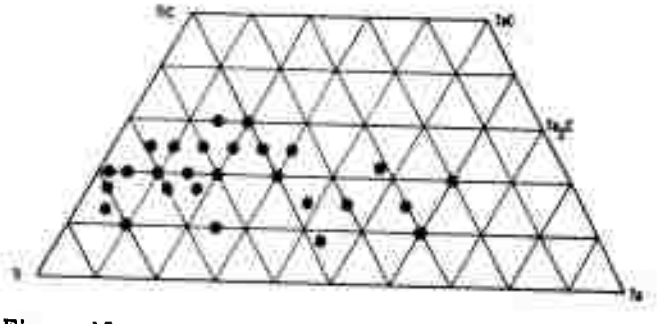

Figure 15. Ti-Ta-C: Location of Arc Melted Samples

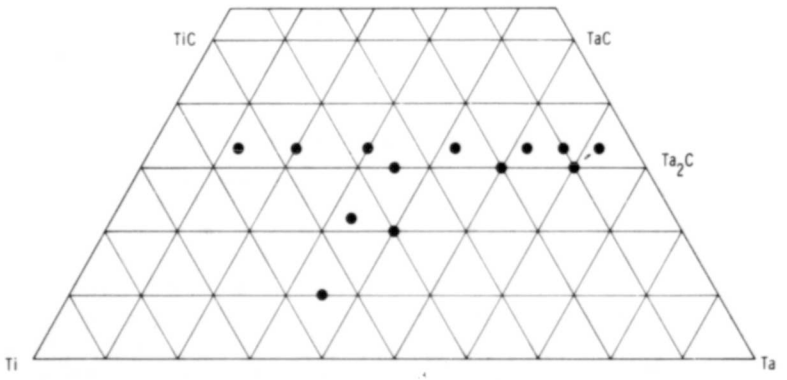

Figure 16. Ti-Ta-C: Location of DTA Samples

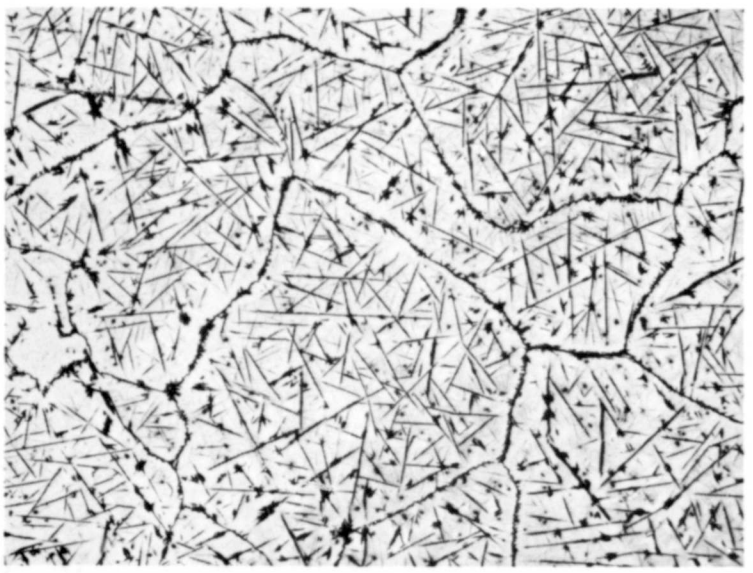

Figure 17. Ti-Ta-C: 55/45/3, Quenched from 2100°C X100
Monocarbide Precipitates (Dark Spikes) Within Metal Grains (Light). Partial Carbide Agglomeration on Grain Boundaries.

was that the small amount of carbide taken into solid solution in the metal phase, was precipitated out on cooling and even on rapid quenching. These carbide precipitates tended to mask further the low carbide-containing eutectic. A series of metallographic pictures depicting the findings along the metal-rich portion of the Ti-Ta-C system are presented in Figures 17 to 26.

The incipient melting points of alloys in the region between 3 and 15 At% carbon correspond to the melting points along the metal-rich eutectic trough. By establishing tie lines connecting the respective incipient melting points of the alloys in this region, it was possible to

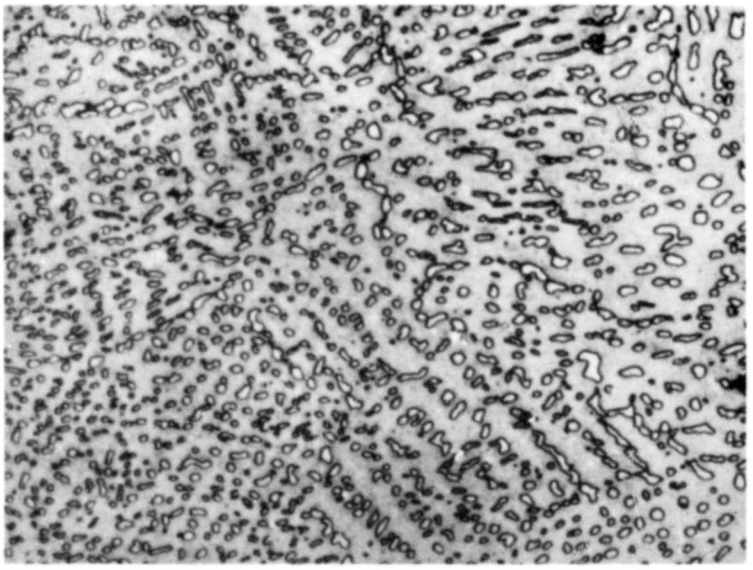

Figure 18. Ti-Ta-C: 53/40/7, Quenched from 2160°C X1000
Fine Monocarbide Primary Crystals (Light) in Metal Matrix (Grey)

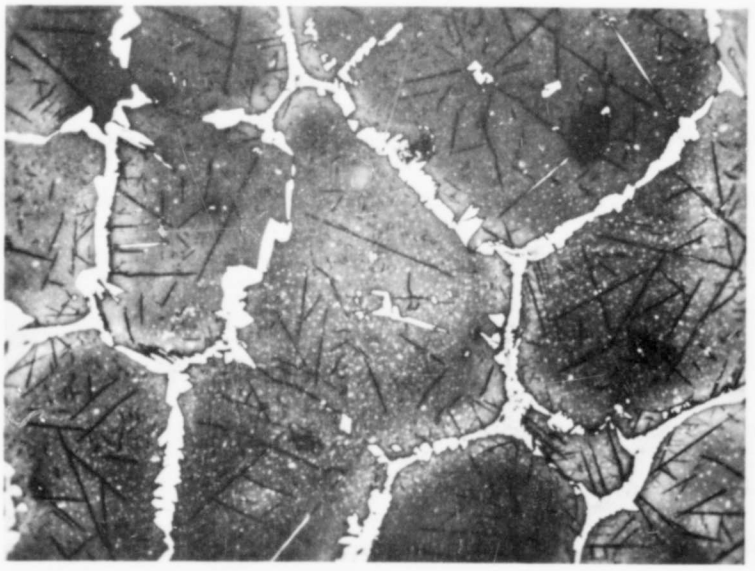

Figure 19. Ti-Ta-C: 35/61/4, Quenched from 2480°C X650

Metal Grains (Grey) Outlined by Agglomerated Subcarbide (Light) Collected on Grain Boundaries. Subcarbide Precipitates (Dark Spikes) Within Metal Grains.

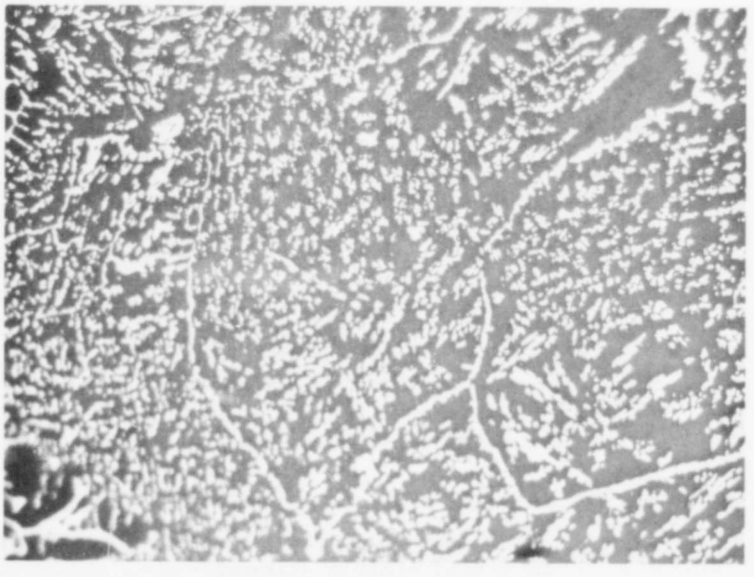

Figure 20. Ti-Ta-C: 20/73/7, Quenched from 2500°C X500

Partial Eutectic-Like Structure: Fine Subcarbide Grains (Light) in Metal (Grey) Matrix. Subcarbide Partially Agglomerated on Grain Boundaries.

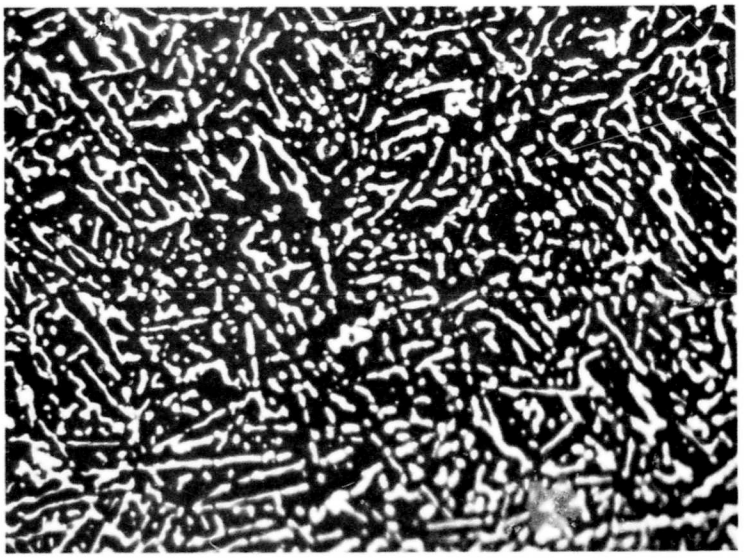

Figure 21. Ti-Ta-C: 20/73/7, Quenched from 2500°C X500

Eutectic-Like Structure: Subcarbide Grains (Light) in Metal Matrix (Grey).

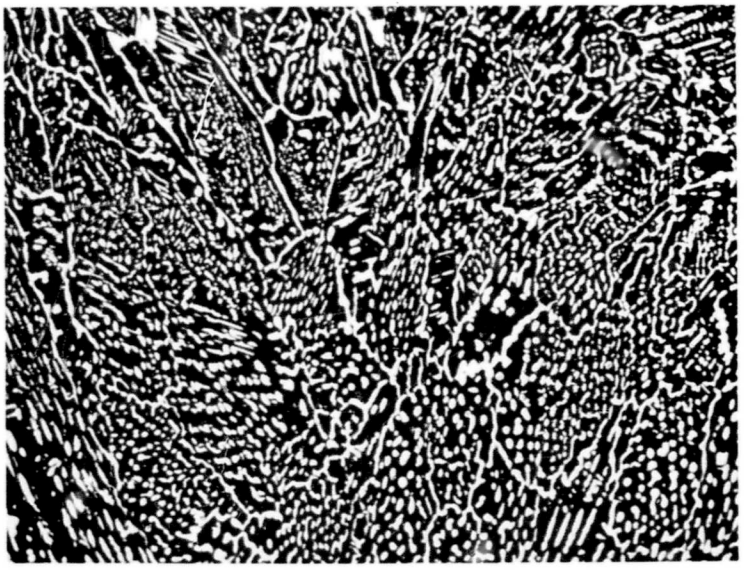

Figure 22. Ti-Ta-C: 10/81/9, Quenched from 2760°C X500

Eutectic-Like Structure: Subcarbide (Light) in Metal Matrix (Dark).

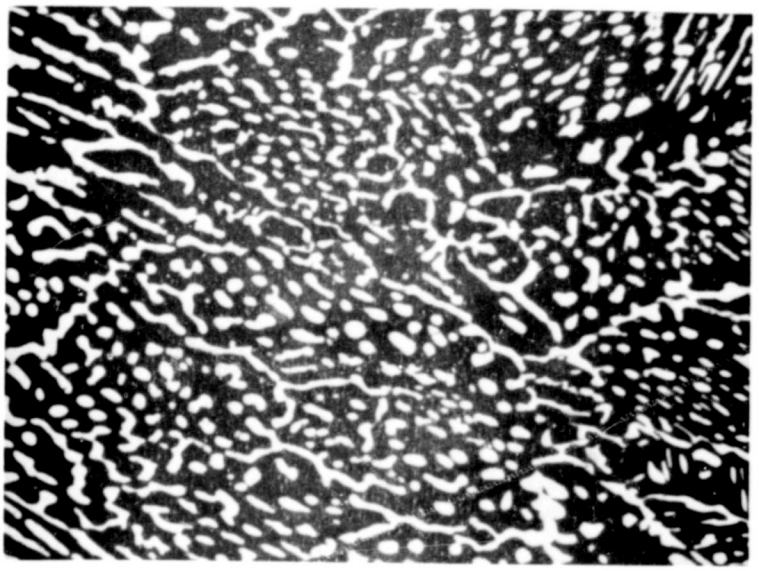

Figure 23. Ti-Ta-C: 10/81/9, Quenched from 2760°C X1000

Eutectic-Like Structure: Subcarbide (Light) in Metal Matrix (Dark).

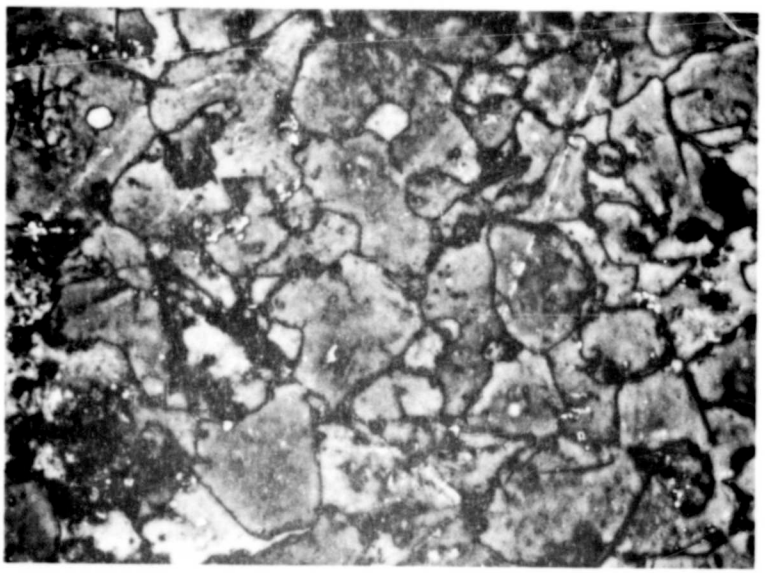

Figure 24. Ti-Ta-C: 60/25/15, Quenched from 1970°C X1000

Primary Monocarbide Grains (Light and Grey) Surrounded by Metal Matrix (Dark)

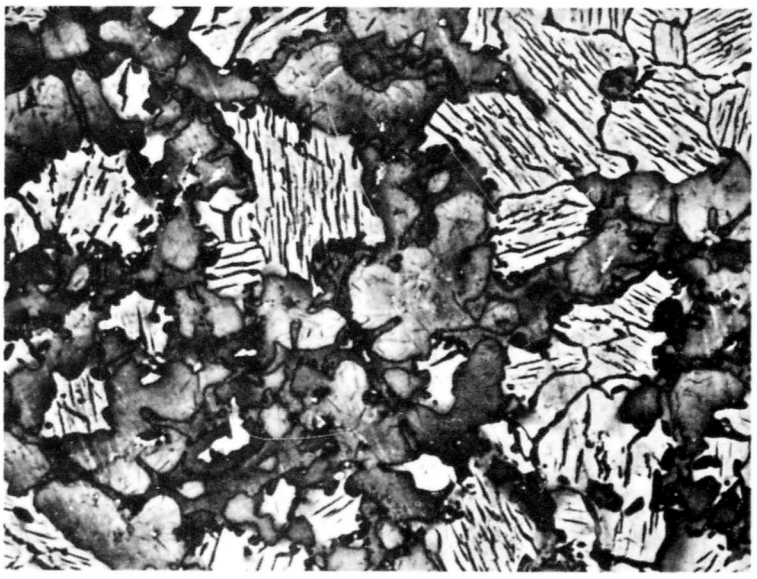

Figure 25. Ti-Ta-C: 40/45-15, Quenched from 2650°C X650

Subcarbide (Large Light Grains with Dark Metal Precipitates Within Grains) and Monocarbide (Small White Grains Without Metal Precipitates) in a Metal Matrix (Grey)Showing Some Fine Carbide Precipitates(Darker Grey).

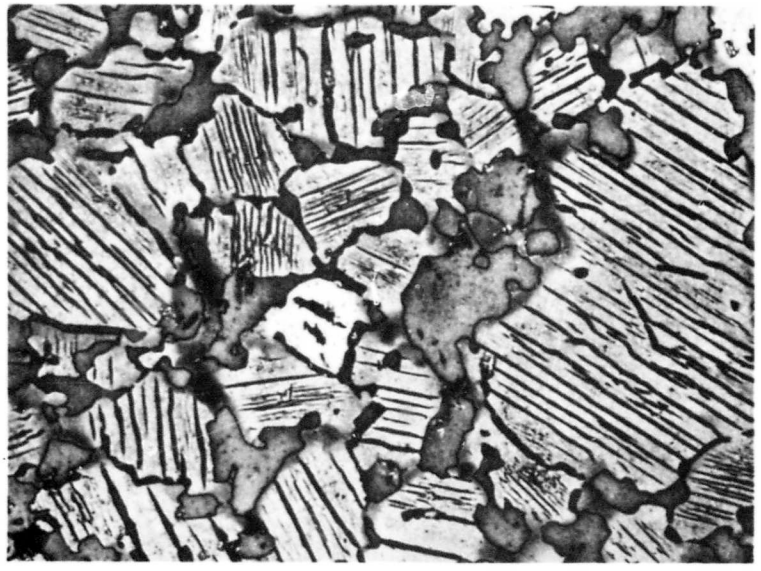

Figure 26. Ti-Ta-C: 30/55/15, Quenched from 2700°C X650

Large Subcarbide (Light) Grains with Heavy Metal Precipitates Within Grains in a Metal (Grey) Matrix.

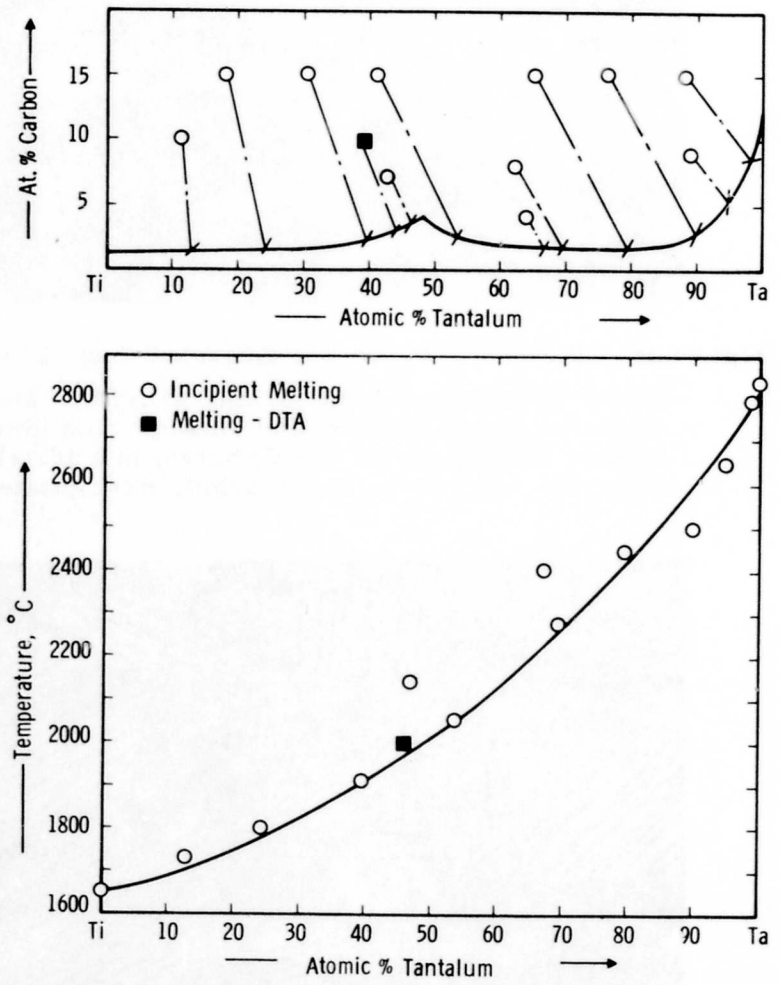

Figure 27. Ti-Ta-C: Tie-Line-Corrected Melting Points and Position of Metal-Rich Eutectic Trough

present a melting point curve of the eutectic trough, although many of the samples chosen do not lie directly on the trough itself. Figure 27 depicts these melting points as a function of the tie-line corrected compositions. The smaller diagram shows the position of the eutectic trough with the tie-line corrections applied. The eutectic trough was positioned with the aid of extensive metallographic investigations (See Figures 17 to 26).

From examination of the collapsing temperatures of samples in the two phase β-(Ta, Ti)$_2$C-(Ta, Ti) region, it was concluded that the peritectic trough, initiating in the Ta-C binary, slides rather quickly to lower carbon concentrations. This path is depicted in conjunction with a liquidus projection of the whole Ti-Ta-C system in Figure 48.

Extensive use of the differential thermal analysis technique made the tracing of the α-β-(Ta, Ti)$_2$C transformation, which begins in the binary Ta-C system, relatively easy. Figure 28 shows a compilation of the information obtained from DTA samples located at 30 and 33 At% carbon.

With increasing amounts of titanium, the β-(Ta, Ti)$_2$C is stabilized to lower temperatures; at 1815°C the β-(Ta, Ti)$_2$C high temperature form decomposes eutectoidally giving rise to a four-phase reaction at this temperature. Also shown in Figure 28 is the plot of points indicating the temperature dependence of the metal-rich β-(Ta, Ti)$_2$C boundary upon the titanium concentration. Finally, the incipient melting points of the alloys at 30 and 33 At% C are also shown in Figure 28.

A series of DTA curves, which contributed in part to the information compiled in Figure 28 is shown in Figures 29 to 32.

The speed of the transformation ($\beta \longrightarrow \alpha$) involved here is easily ascertained by relating the cooling speeds to the type of peak

developed. At these carbon concentrations (30 and 33 At% C) the reaction involves very little tantalum metal phase, and the reaction is mainly the transformation of the β-$(Ta, Ti)_2C$ to α-$(Ta, Ti)_2C$. The sharper the peak is at fast cooling speeds, the more rapid the physical transformation is. The sharp peaks of the curves at the rapid cooling speeds show that the β-α-transformation occurs quite quickly, although X-ray findings (diffuse patterns) indicate that the transformation is not of the martensitic type.

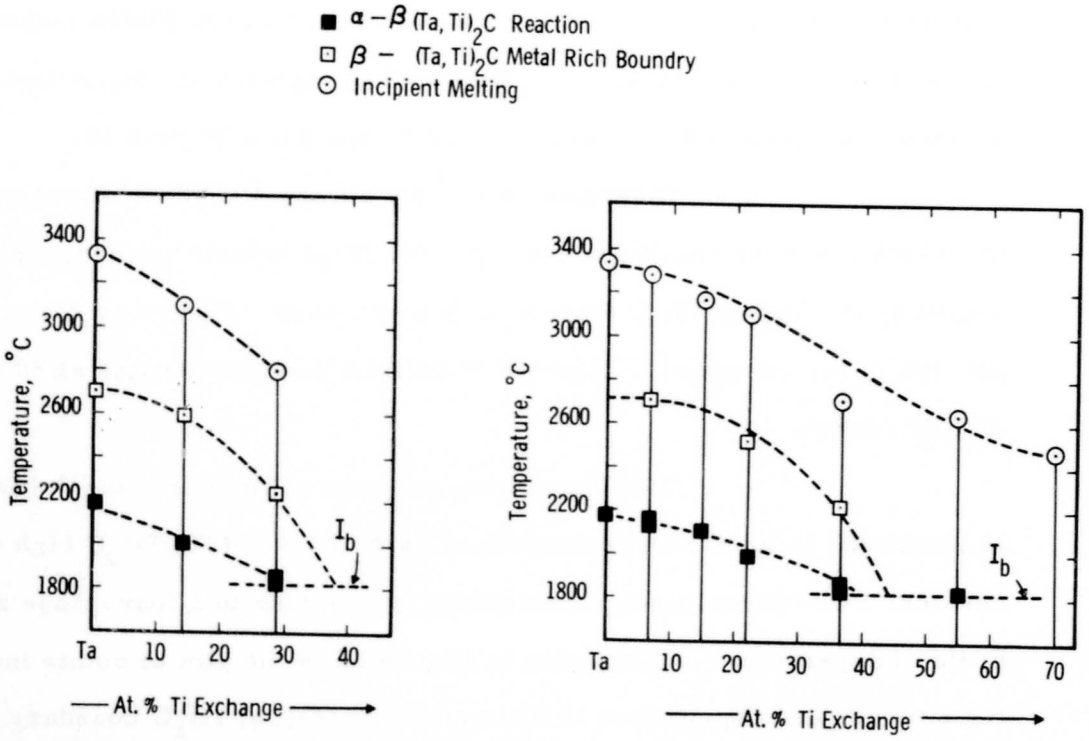

Figure 28. Ti-Ta-C: Temperature Variance of α-β $(Ta, Ti)_2C$ Reaction, β-Metal-Rich Phase Boundary, and Melting Points of DTA Samples with 30 and 33 At% Carbon at Various Titanium Concentrations.

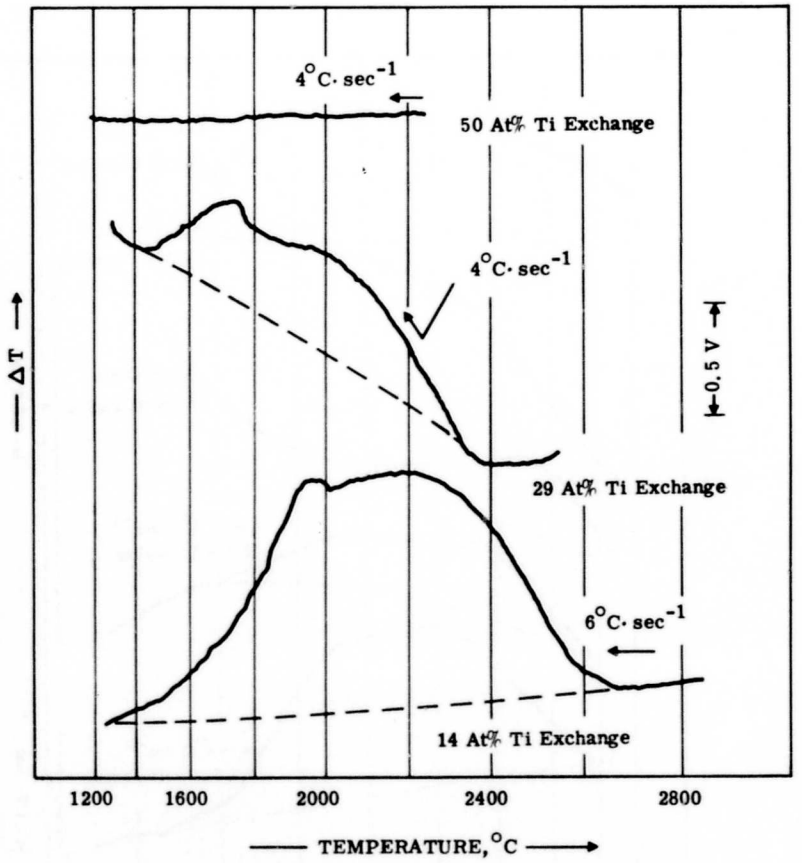

Figure 29. Ti-Ta-C: Differential Cooling Curves at 30 At% Carbon with 14 - 50 At% Titanium Exchange α-β-$(Ta, Ti)_2C$ Reaction Under Moderate Cooling Conditions.

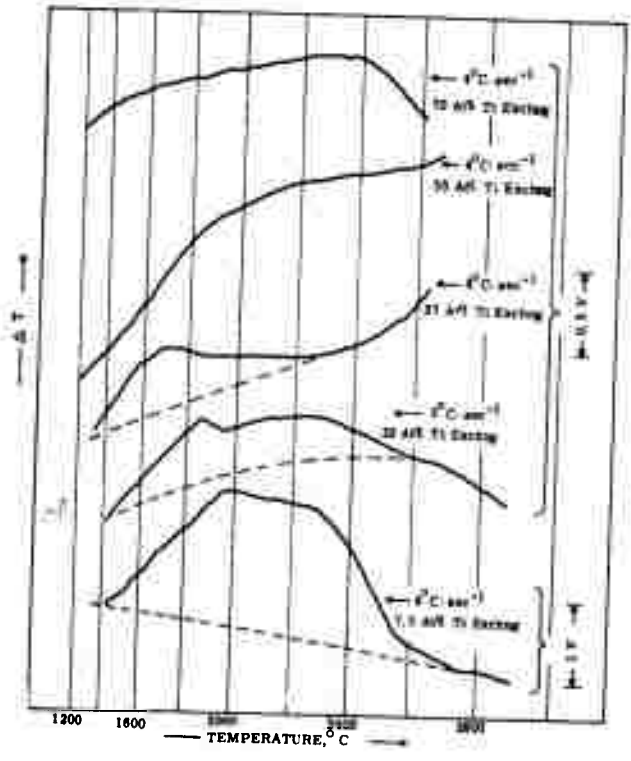

Figure 30. Ti-Ta-C: Differential Cooling Curves at 33 At% Carbon with 7.5-70 At% Titanium Exchange α-β-$(Ta, Ti)_2C$ Reaction Under Moderate Cooling Conditions.

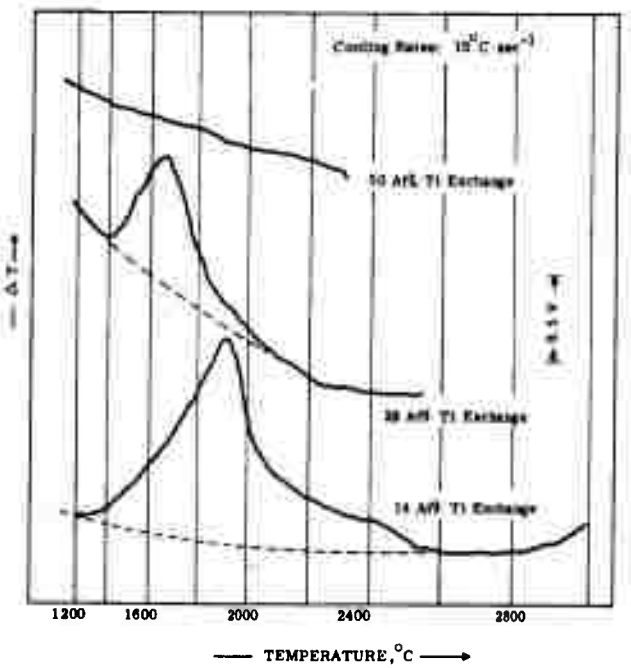

Figure 31. Ti-Ta-C: Differential Cooling Curves at 30 At% Carbon with 14 - 50 At% Titanium Exchange

α-β-$(Ta, Ti)_2C$ Reaction Under Rapid Cooling Conditions

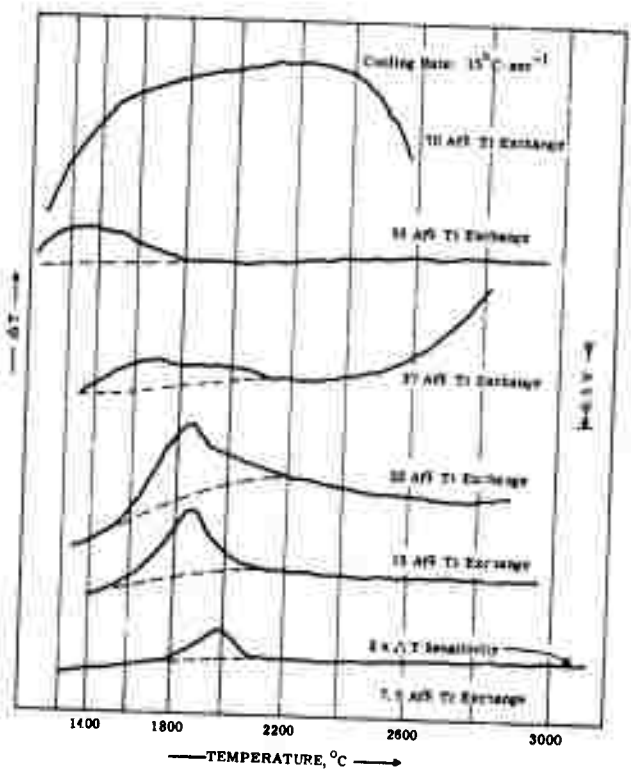

Figure 32. Ti-Ta-C: Differential Cooling Curves at 33 At% Carbon with 7.5 - 70 At% Titanium Exchange.

α-β-$(Ta, Ti)_2C$ Reaction Under Rapid Cooling Conditions

There are but two possible reactions involving the α-β subcarbides which might occur at the four phase reaction plane at 1815°C where the α-$(Ta, Ti)_2C$ reaches its maximum solubility for "Ti_2C".

The first possibility is the termination toward the ternary (titanium-richer field) of the β-$(Ta, Ti)_2C$ (γ') solid solution by a Class II four-phase reaction according to:

$$\gamma' + \beta \rightleftharpoons \gamma + \delta$$

followed by a quasi-binary eutectoid reaction isotherm where the β-$(Ta, Ti)_2C$ (γ') completely vanishes to a limiting tie line at some intermediate composition and at a temperature lower than that of the four-phase reaction plane.

The eutectoid reaction would be

$$\gamma' \rightleftharpoons \gamma + \delta$$

Progressing from higher to lower temperatures, Figures 33 to 36 schematically show this possible four-phase reaction and the ensuing eutectoid decomposition.

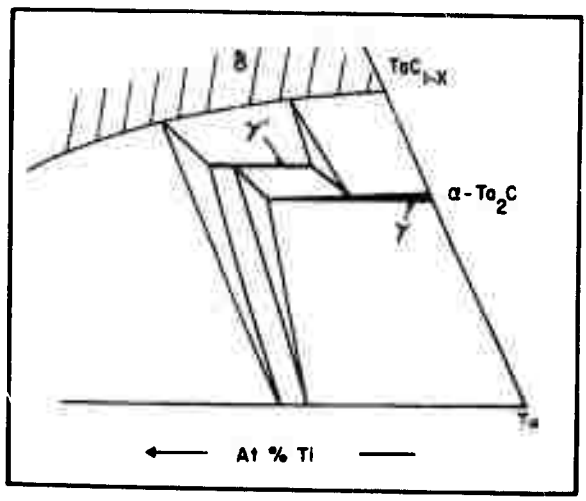

Figure 33. Ti-Ta-C: Schematic Illustration of Phase Equilibria Above Four-Phase Reaction Plane According to First Possibility.

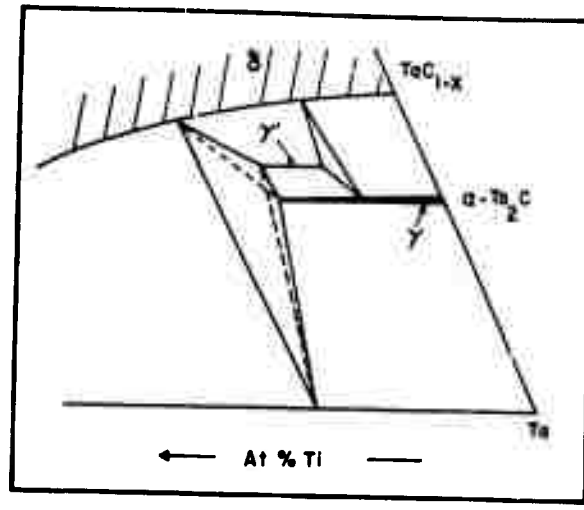

Figure 34. Ti-Ta-C: Schematic Illustration of Four-Phase Reaction Plane According to First Possibility:

$$\gamma' + \beta \rightleftharpoons \gamma + \delta$$

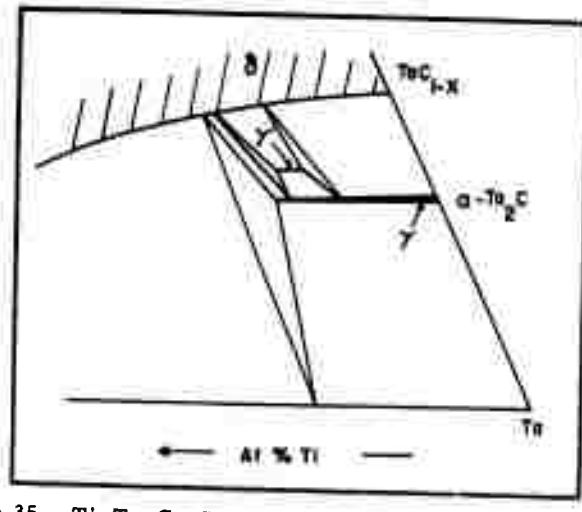

Figure 35. Ti-Ta-C: Schematic Illustration of Phase Equilibria Below Four-Phase Reaction Plane According to First Possibility.

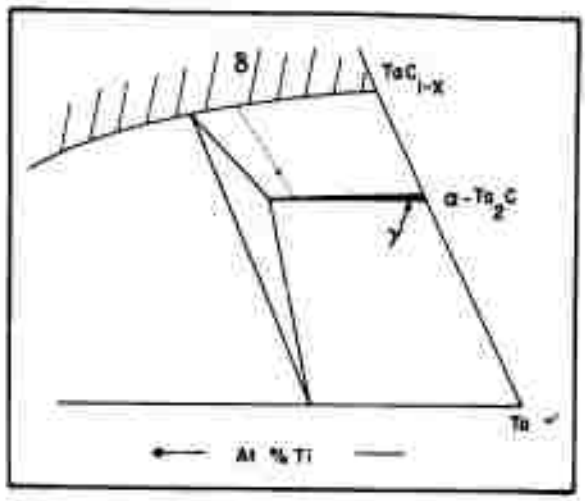

Figure 36. Ti-Ta-C: Schematic Illustration of Phase Equilibria Below Four-Phase Reaction Plane According to First Possibility. Disappearance of β-$(Ta, Ti)_2C$ into a Limiting Tie Line.

The second possibility is the termination of the β-$(Ta, Ti)_2C$ (γ') solid solution by a Class I four-phase eutectoid reaction according to:

$$\gamma' \rightleftharpoons \gamma + \beta + \delta$$

Figure 37 shows an exploded isometric view of the four-phase reaction plane according to the second possibility. Isotherms indicating the phase equilibria above, at, and below the second type of four-phase plane are found in Figures 50 to 52.

Both four-phase reaction plane possibilities are equally probable, and both would explain the reactions at the four-phase plane.

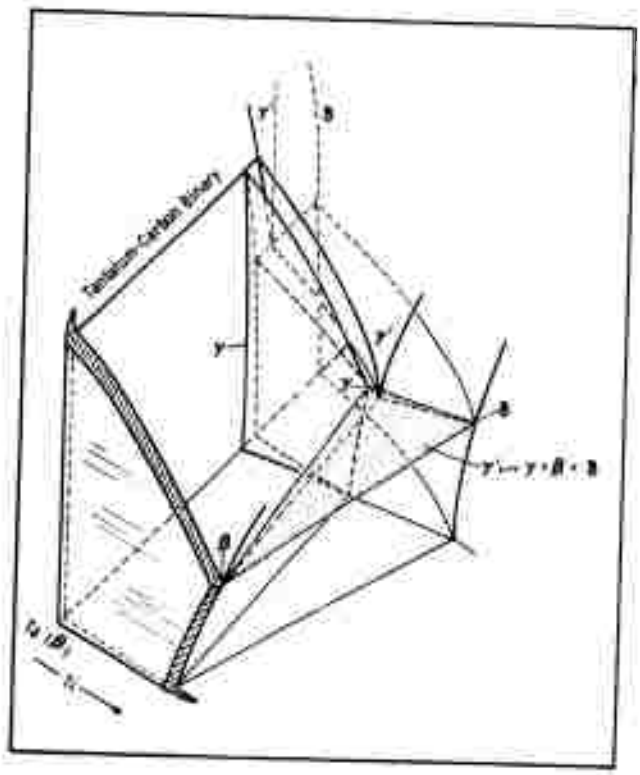

Figure 37. Ti-Ta-C: Exploded Isometric View of the Class I_b Four-Phase Reaction Plane.

The second possibility, the eutectoid reaction according to: $\gamma' \rightleftharpoons \gamma + \delta + \beta$ was given preference.

With increasing temperature the β-Ta_2C takes increasing amounts of "Ti_2C" into solid solution; concurrently the liquid area, which leads along the metal-rich eutectic trough, gradually progresses toward the center of the diagram (Figures 51 to 53).

When the results of the X-ray analysis of samples with 15 or less atomic percent carbon, which were used for melting point measurements, were compared with those of solid state samples in the two-phase $(Ti, Ta)_2C_{1-x}$-(Ti, Ta) region, it was seen that samples lying outside the solid state β-$(Ta, Ti)_2C$-$(Ti, Ta)C_{1-x}$-(Ta, Ti) three-phase region suddenly showed considerable amounts of the β-$(Ta, Ti)_2C$ phase.

To confirm the already indicated four-phase reaction and to ascertain the reaction plane's temperature, DTA samples in this region (Figures 16 and 54) were investigated. The results determined that the Class II four-phase reaction involving the liquid on the eutectic trough occurs at 2020 $\pm$ 15°C according to:

$$\gamma' + L \rightleftharpoons \delta + \beta$$

Figure 38 portrays a DTA cooling curve of one of the alloys in the four-phase quadrant.

A superpositioning of the four-phase quadrant boundary line, $(Ti, Ta)C_{1-x}$-Liquid, determined by qualitative X-ray analysis of the melting point samples, onto the melting temperature vs. composition plot of the metal-rich eutectic gave a four-phase plane reaction temperature of about 1970°C. This determination is in fairly close agreement with the

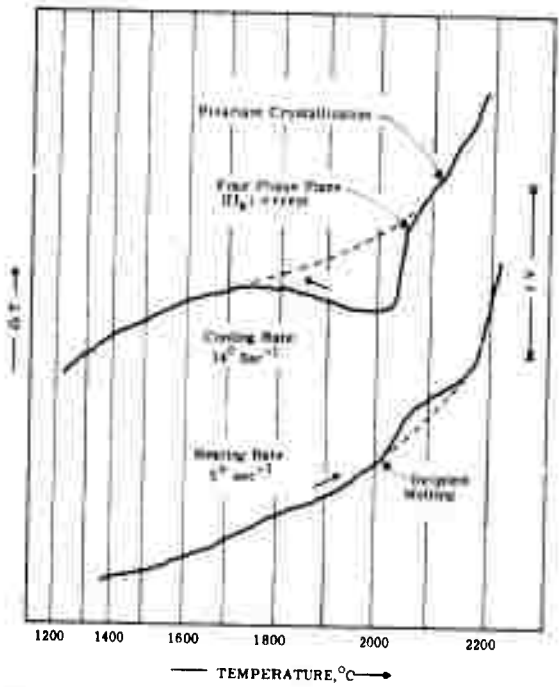

Figure 38. Ti-Ta-C: 45/23/32 DTA Heating and Cooling Curves of an Alloy in the Four-Phase Reaction (II_a) Quadrant

far more accurate temperature of 2020°C determined from DTA cooling curves. In addition, the four-phase reaction temperature determined here is in excellent agreement with the 2025°C determined by J. T. Norton[31] on samples metallographically investigated for incipient melting.

Figures 53 to 55 show the phase relationships below, at, and above this four-phase plane.

The X-ray and metallographic analysis of samples near the metal-rich monocarbide boundary, on the titanium-rich side, which were quenched from temperatures between 2600° and 3050°C, indicated that the metal-rich boundary of the monocarbide does not differ greatly from its location at lower temperatures. No metal precipitates were observed in the monocarbide grains (Figures 39 and 40).

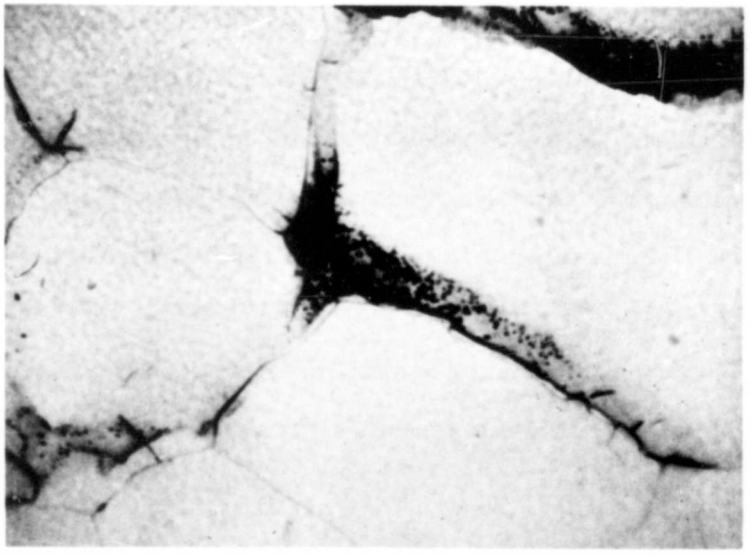

Figure 39. Ti-Ta-C: 53/12/35, Quenched from 3050°C X1000
Large Monocarbide Grains(Light) With Small Amounts of Metal(Grey and Black)Phase at the Grain Boundaries

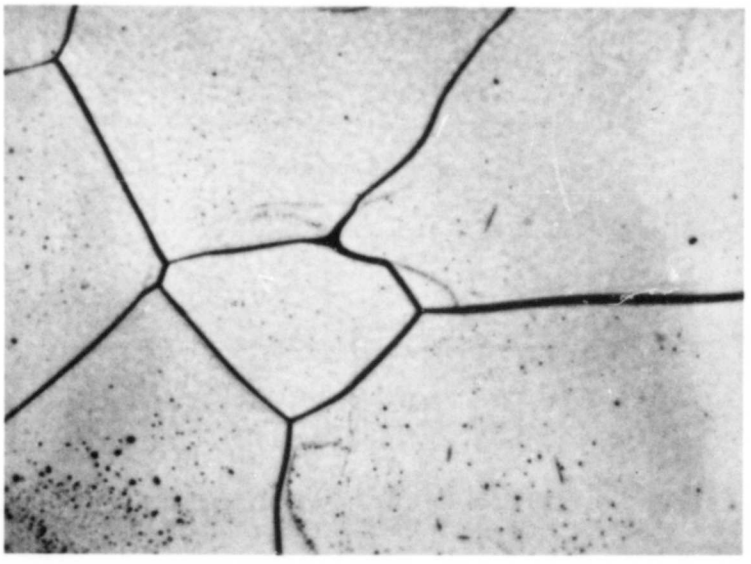

Figure 40. Ti-Ta-C: 60/5/35, Quenched from 3025°C.
Single Phase Monocarbide

The carbon-rich boundary of the monocarbide solid solution is located at slightly hypostoichiometric compositions over the whole range of metal concentrations. At higher temperatures, the carbon defect, approximately 6 At% C at the melting point of $TiC_{0.79}$, decreases along a smooth boundary toward the tantalum side. No free-carbon analyses from samples in this high temperature range were available; however, no significant changes indicating a deviation from a smooth boundary line connecting the binary solubility limits at the respective temperatures were indicated. Figure 41 shows the solidus temperatures of (Ta, Ti)C alloys at 45 At% C.

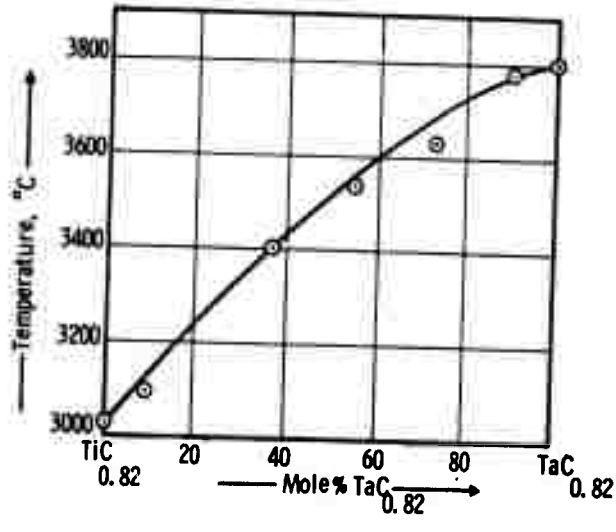

Figure 41. Ti-Ta-C: Solidus Curve of (Ta, Ti)$C_{0.82}$ Alloys

The melting temperatures of the carbon-rich eutectic trough were measured on five ternary samples containing 60 and 65 At.% carbon (Figure 14). The samples melted fairly sharply indicating that the eutectic trough does not lie very far away from the location of the samples. The melting points (Figure 42) were found to lie along an almost linear curve connecting the $TaC_{0.99}$-C and $TiC_{0.94}$-C binary eutectics at 3445°C and 2776°C respectively. Figures 43 and 44 show the metallographic results of alloys in the carbon-rich region.

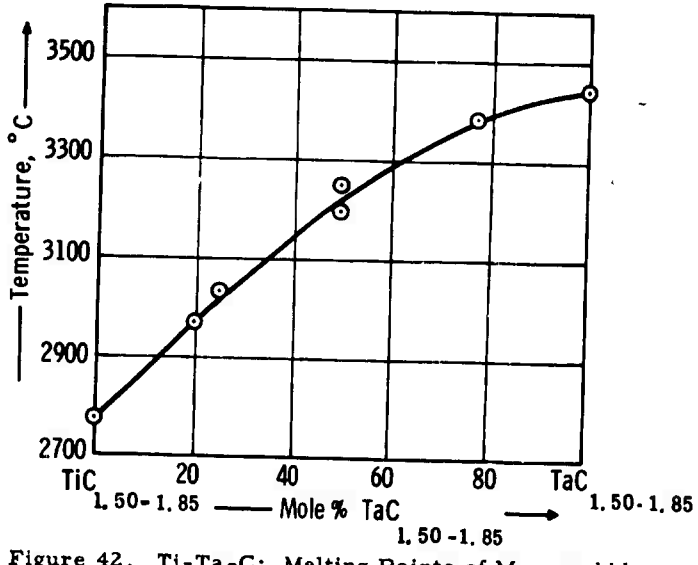

Figure 42. Ti-Ta-C: Melting Points of Monocarbide-Graphite Eutectic

The experimental evidence obtained in all the investigations of the Ti-Ta-C System is compiled in a three-dimensional space model diagram presented in Figure 45. Since the reaction rates at lower temperatures are expected to be extremely slow, with the exception of the α-β-titanium transition which was not investigated in detail, no experimental investigations were carried out below 1000°C.

Figure 43. Ti-Ta-C: 19/19/62 Quenched from 3300°C X100
Primary Graphite Needles in Eutectic Graphite-Carbide Matrix.

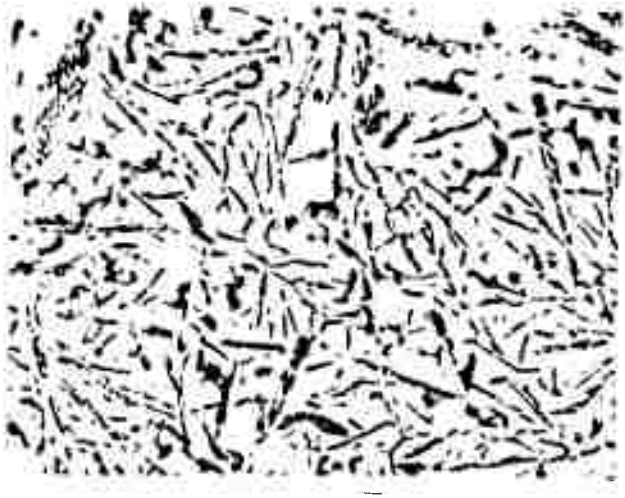

Figure 44. Ti-Ta-C: 20/20/60 Quenched from 3200°C X100
Carbon-Graphite Eutectic Structure

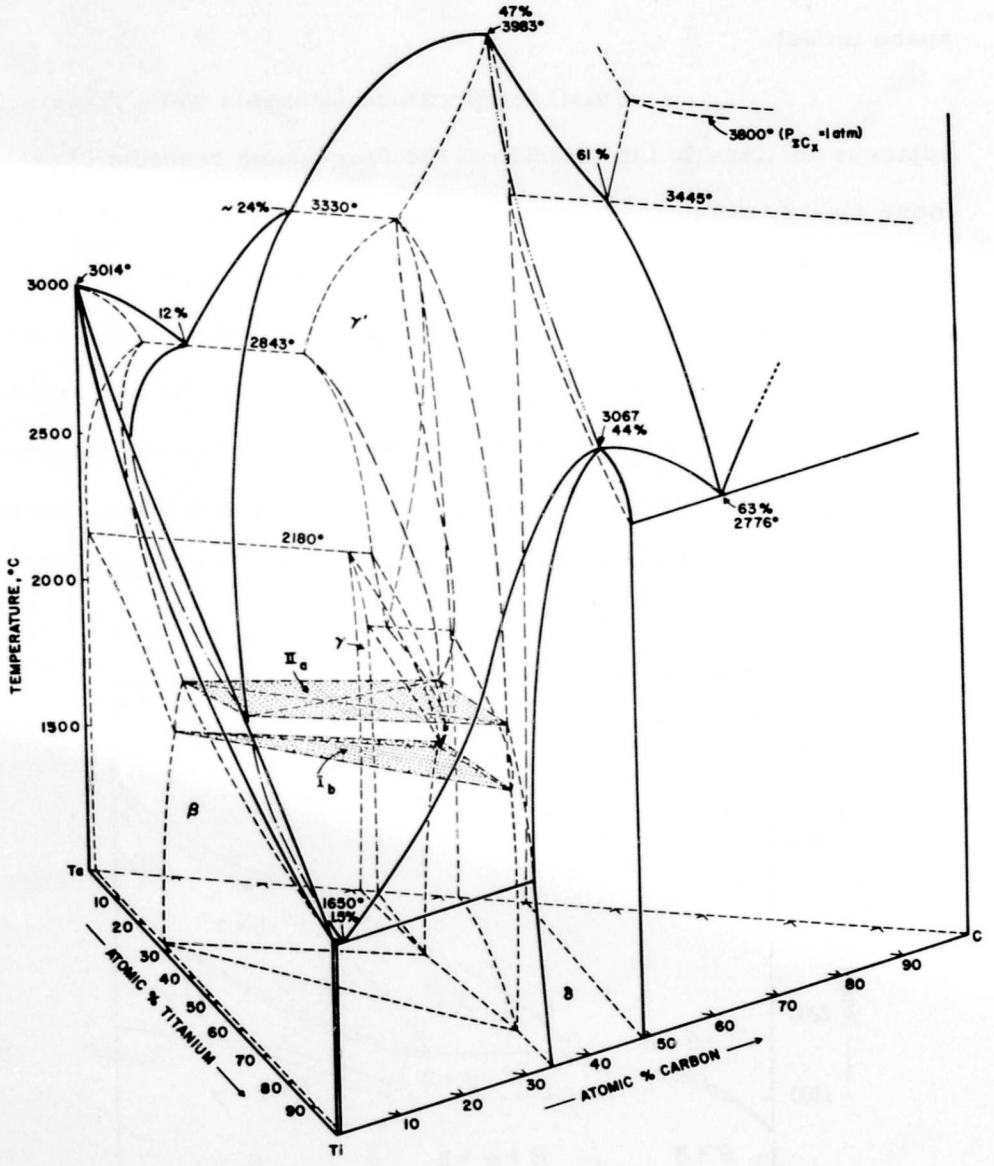

Figure 45. Ti-Ta-C: Three-Dimensional Space Model

A series of temperature sections from 1500°C to 3800°C are presented in Figures 49 to 63 to aid in the visualization of the space model.

Small temperature intervals were taken with several adjacent sections in the vicinity of the four-phase reaction phases to depict more clearly the phase equilibria near these temperatures. One isopleth, at 30 At% C, (Figure 46) containing the equilibria of the metal-rich portion of the ternary Ti-Ta-C system is also presented; should the need for further isopleths arise, they may be easily developed from the temperature sections.

The invariant and univariant (p = const.) reactions occurring in the ternary Ti-Ta-C system, along with those reactions of the corresponding binary systems, are compiled in a Scheil-Schultz diagram shown in Figure 47.

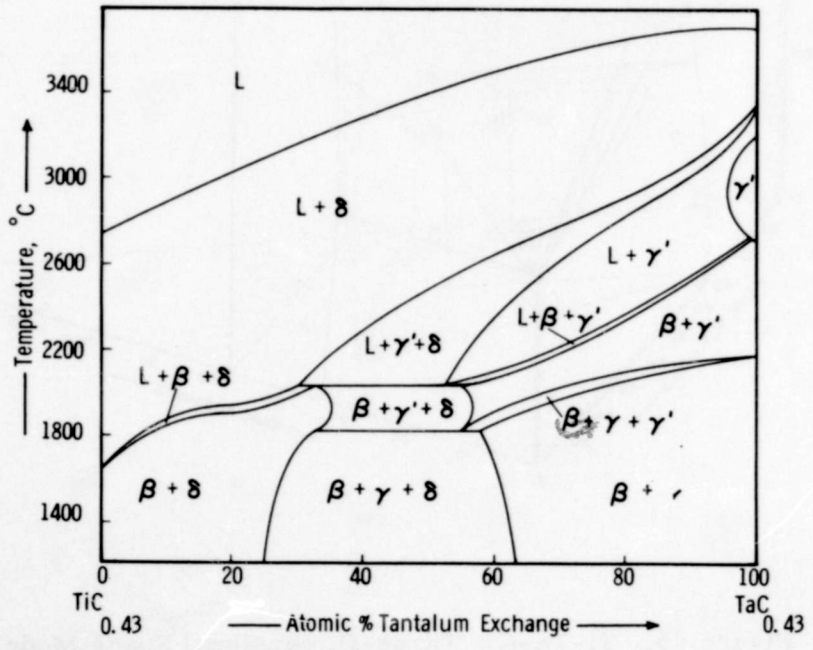

Figure 46. Ti-Ta-C: Isopleth at 30 At% Carbon

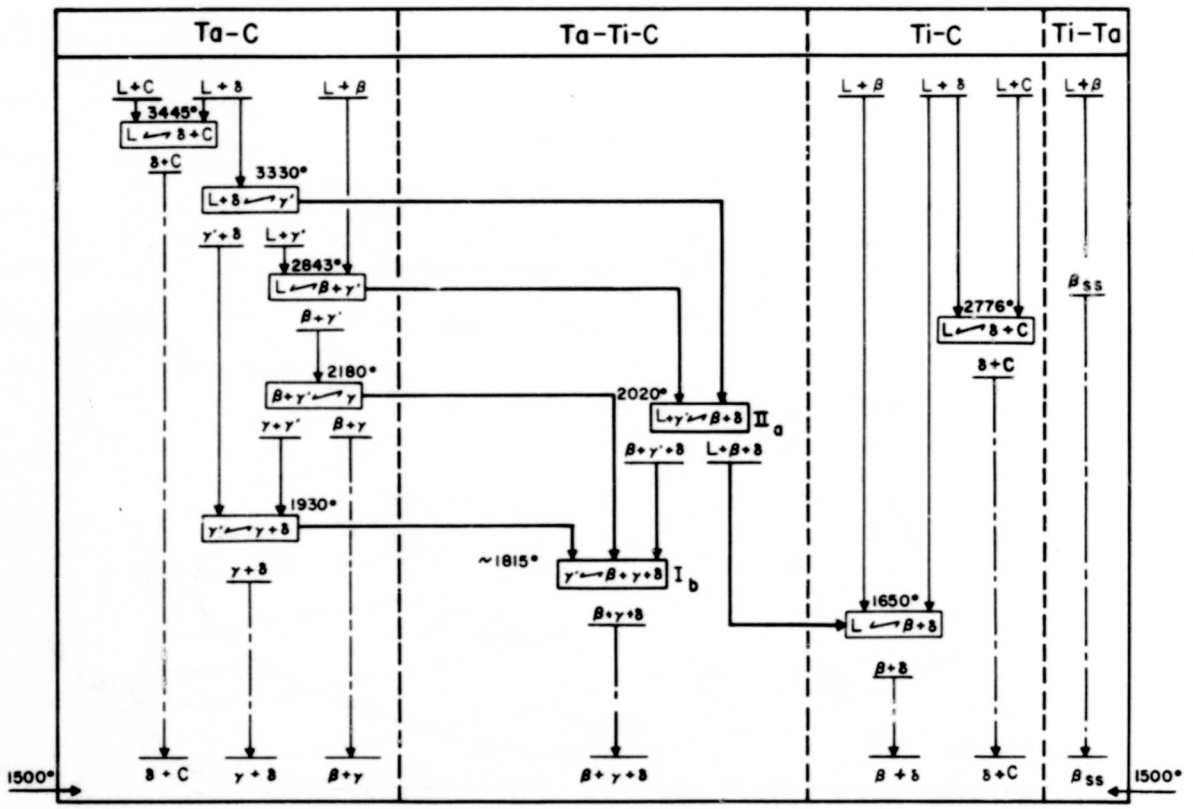

Figure 47. Ti-Ta-C: Scheil-Schultz Diagram

A diagram showing the liquidus curves of the entire Ti-Ta-C system is presented in Figure 48 as a final supplement to the phase equilibrium data.

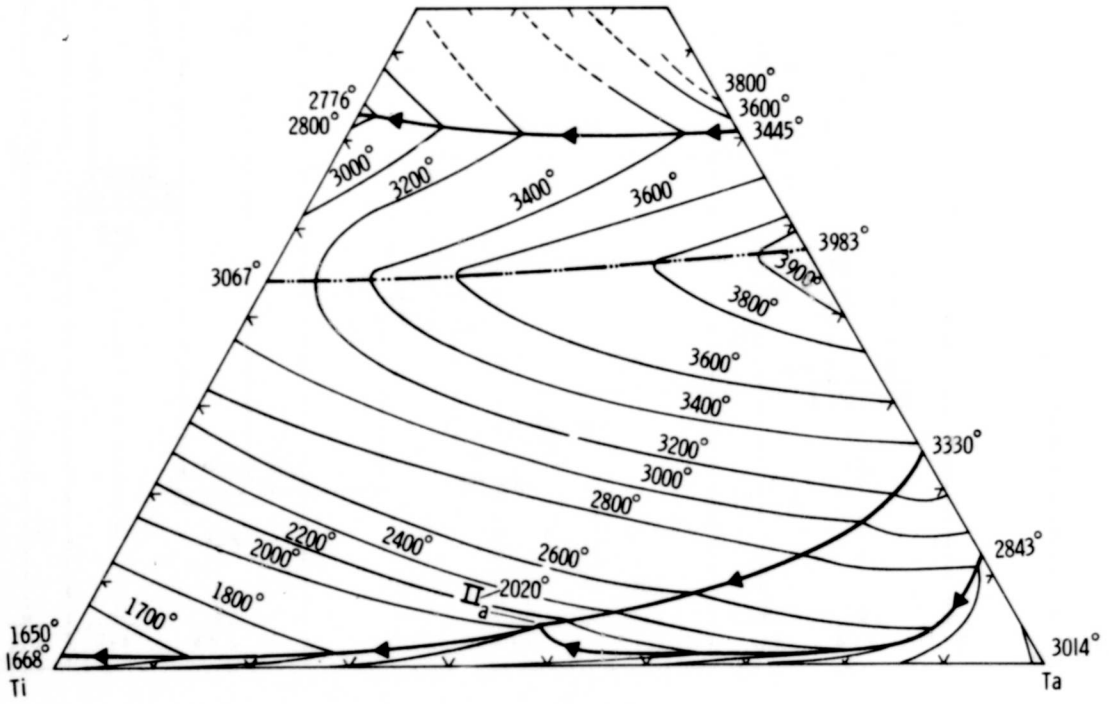

Figure 48. Ti-Ta-C: Liquidus Projection of

—·—·— **Maximum Solidus of Monocarbide Solid Solution.**

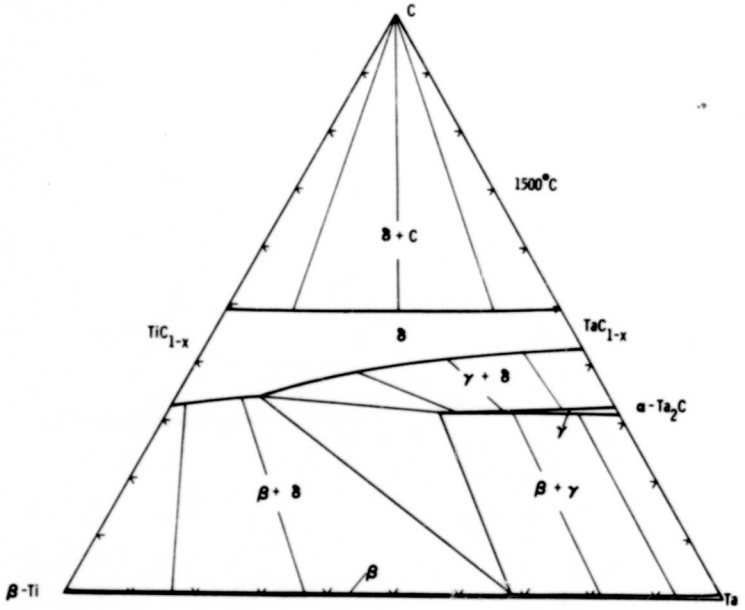

Figure 49. Ti-Ta-C: Isothermal Section at 1500°C

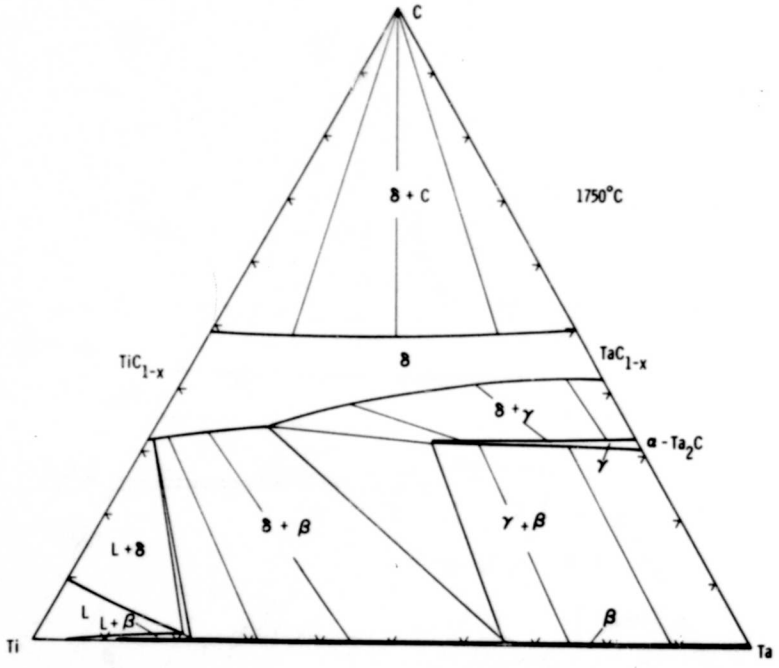

Figure 50. Ti-Ta-C: Isothermal Section at 1750°C

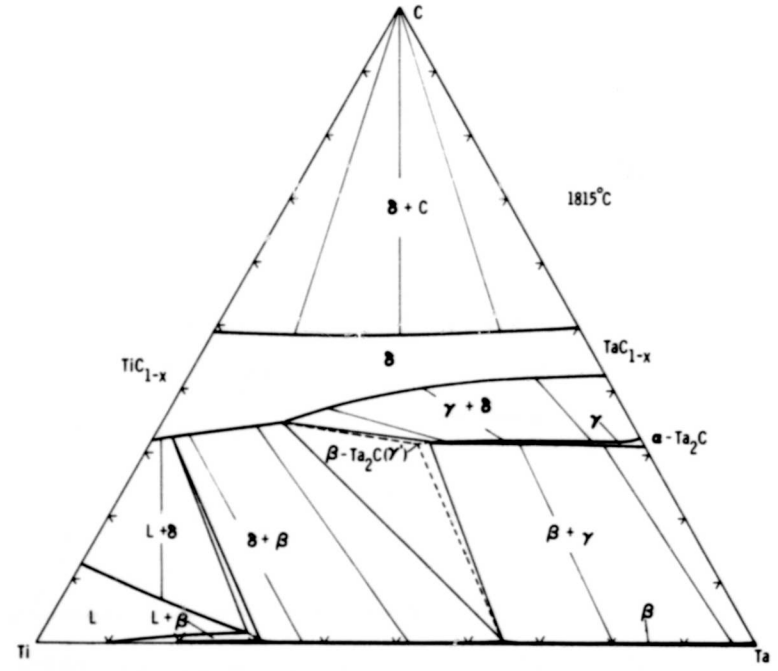

Figure 51. Ti-Ta-C: Isothermal Section at 1815°C

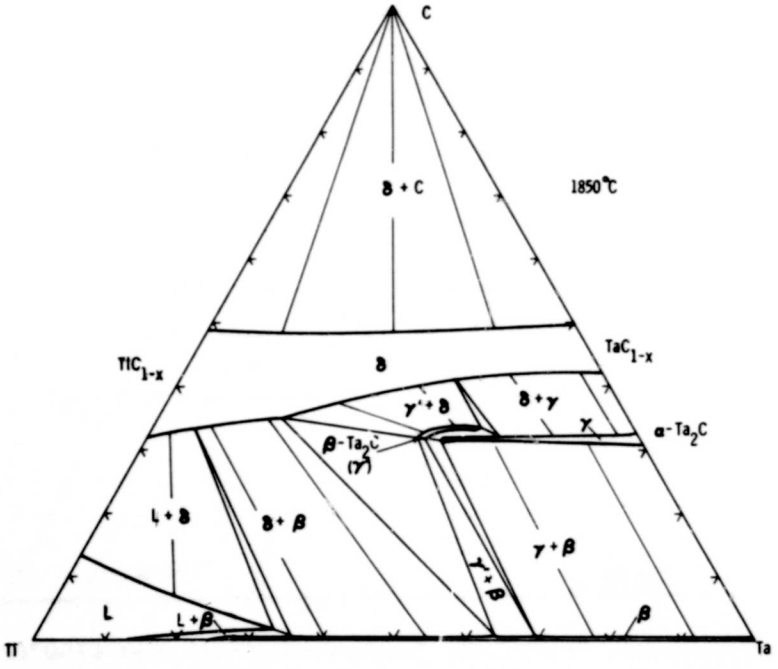

Figure 52. Ti-Ta-C: Isothermal Section at 1850°C

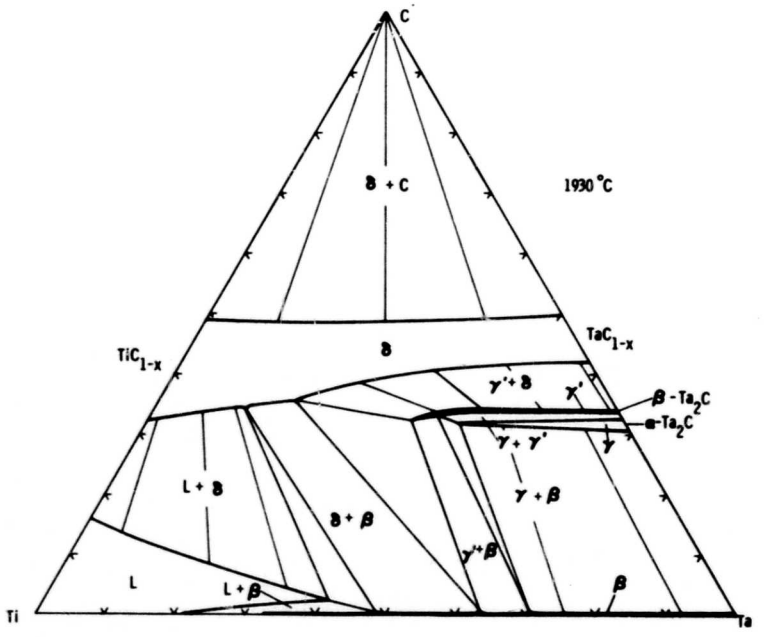

Figure 53. Ti-Ta-C: Isothermal Section at 1930°C

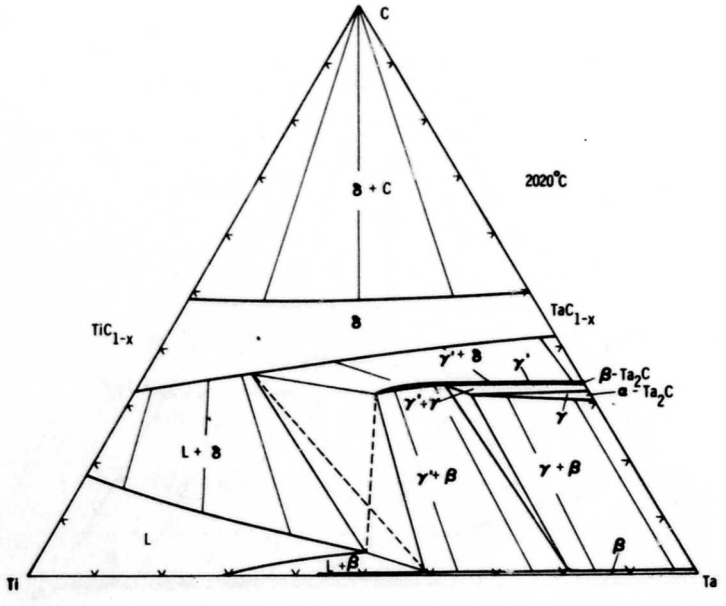

Figure 54. Ti-Ta-C: Isothermal Section at 2020°C

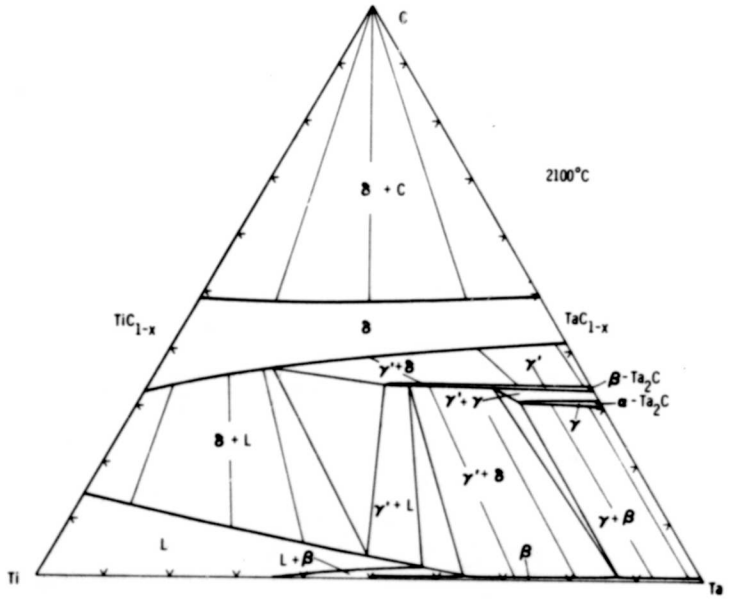

Figure 55. Ti-Ta-C: Isothermal Section at 2100°C

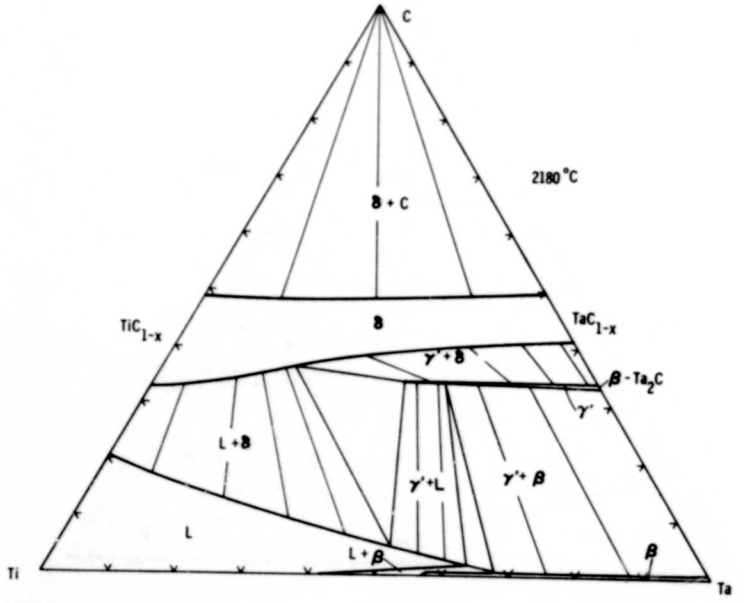

Figure 56. Ti-Ta-C: Isothermal Section at 2180°C

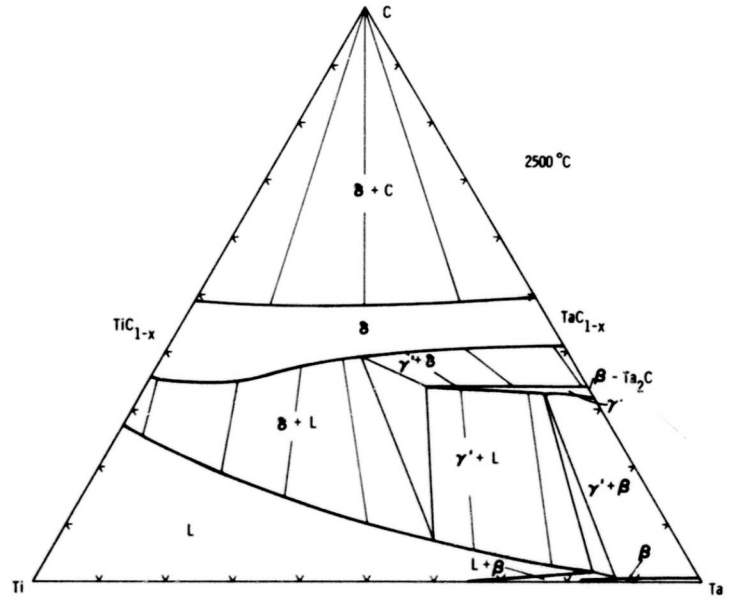

Figure 57. Ti-Ta-C: Isothermal Section at 2500°C

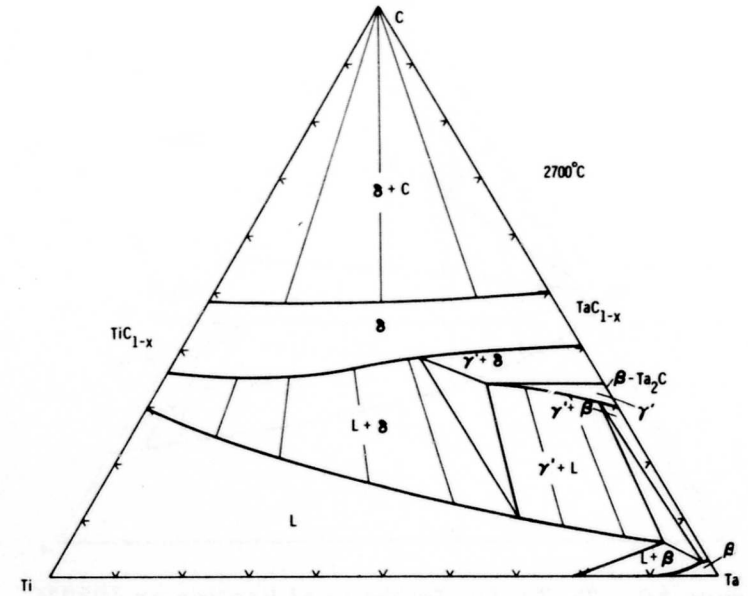

Figure 58. Ti-Ta-C: Isothermal Section at 2700°C

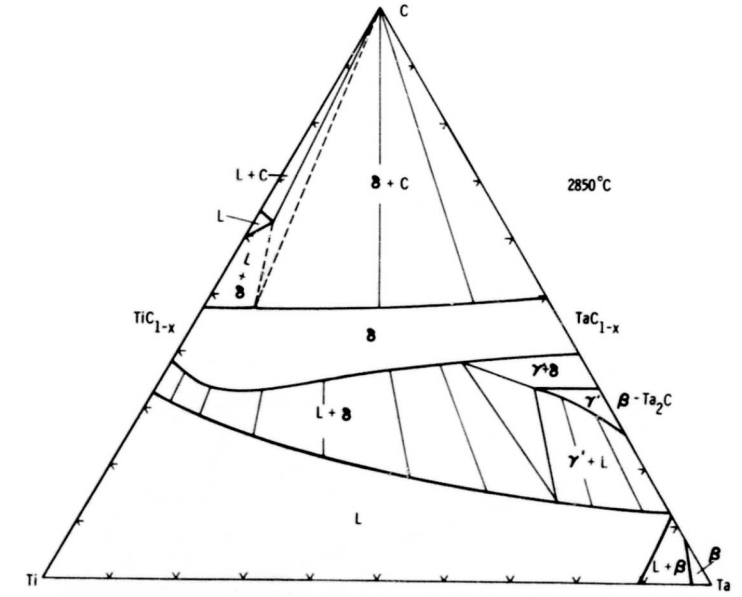

Figure 59. Ti-Ta-C: Isothermal Section at 2850°C

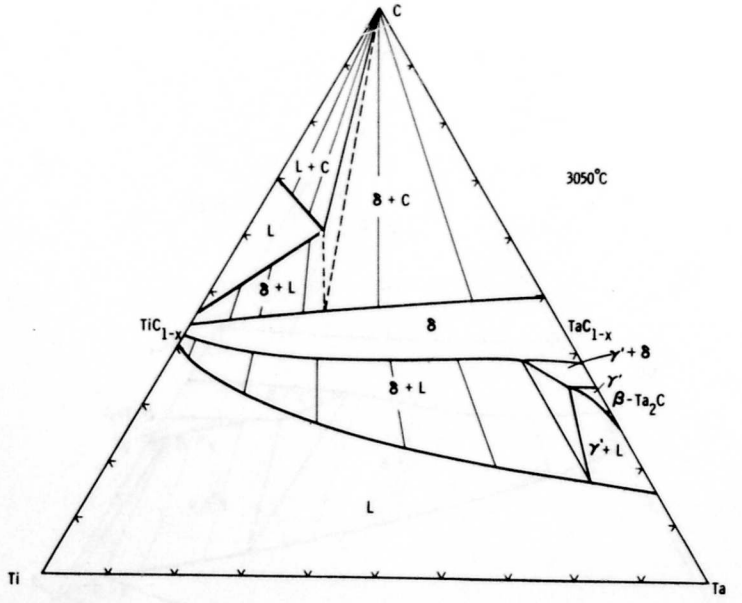

Figure 60. Ti-Ta-C: Isothermal Section at 3050°C

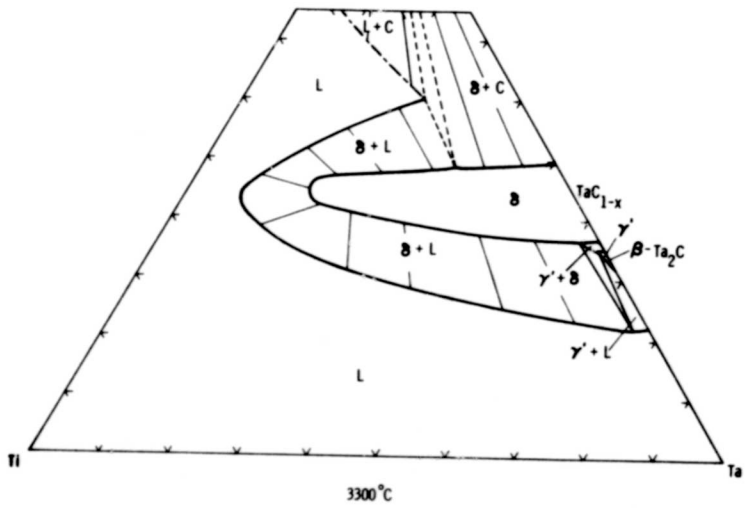

Figure 61. Ti-Ta-C: Isothermal Section at 3300°C

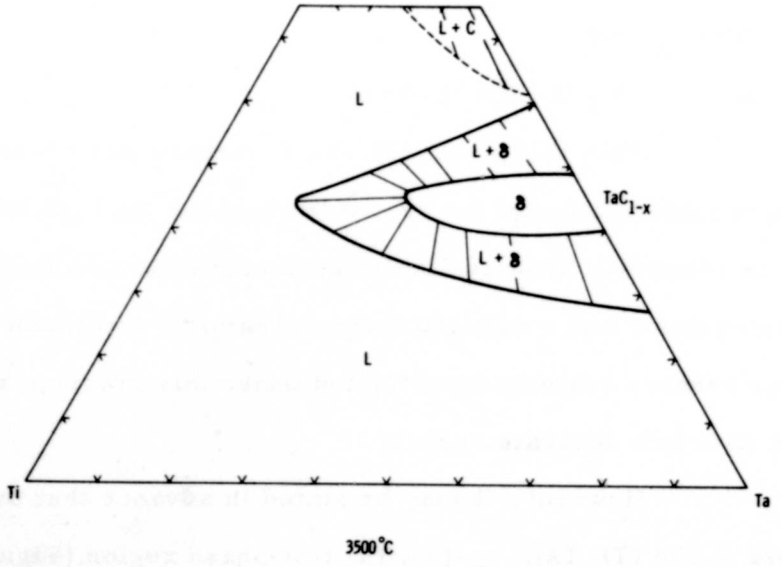

Figure 62. Ti-Ta-C: Isothermal Section at 3500°C

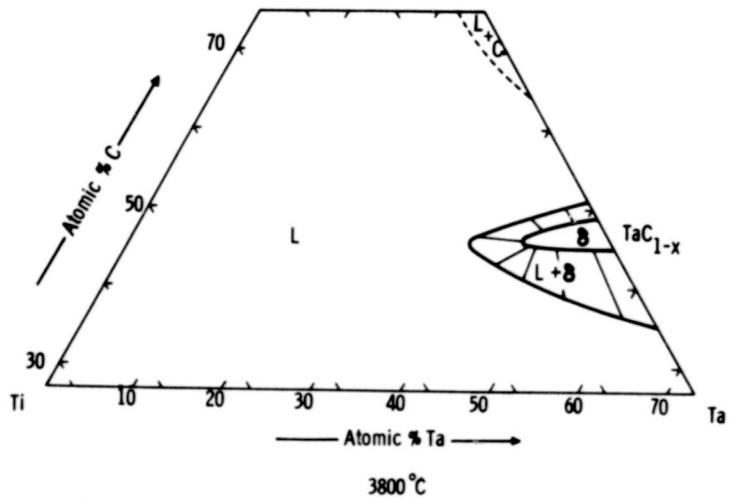

Figure 63. Ti-Ta-C: Isothermal Section at 3800°C

IV. DISCUSSION

A. PHASE EQUILIBRIA

This study of the Ti-Ta-C ternary system is the first extensive investigation of the system throughout the high temperature range. There is relatively little available thermodynamic data concerning the ternary system, and a detailed thermodynamical treatment of this as well as other ternary systems investigated under this program will be given at a later date in a separate report.

However, it may be stated in advance that the slope of the tie lines in the $(Ti, Ta)C_{1-x}$-(Ti, Ta) two-phase region (Figures 49 through 54) confirm the fact that titanium monocarbide, compared to tantalum carbide, has the more negative free energy of formation. Going one step further, titanium carbide, however, has a less negative free energy of formation than hafnium carbide.

A calculation, at 1600°C, using values known[36] for the stoichiometric monocarbides, yielded a free energy difference between TaC and TiC of:

$$\Delta G_f(TiC) - \Delta G_f(TaC) \simeq -3,330 \text{ cal/mol}$$

In comparison, the free energy difference obtained from hafnium carbide and tantalum carbide[37] is:

$$\Delta G_f(HfC_{0.82}) - \Delta G_f(TaC_{0.82}) \simeq -8,500 \text{ cal/mol}$$

In other words, hafnium carbide is more stable than titanium carbide. This fact is expressed when a comparison is made between the slopes of the tie lines in the $(Hf, Ta)C_{1-x}$-(Ta, Hf) two-phase region[38] with those slopes of the tie lines in the corresponding Ti-Ta-C region.

The tie lines in the $(Ti, Ta)C_{1-x}$-(Ti, Ta) region are far less inclined than those in the Hf-Ta-C system, showing the lower stability of titanium carbide compared with hafnium carbide. That is to say, the hafnium-tantalum monocarbide phase of a two-phase alloy in the $(Hf, Ta)C_{1-x}$-(Ta, Hf) region contains far more hafnium than the titanium-tantalum monocarbide phase contains titanium in a comparable Ti-Ta-C two-phase alloy.

Both the α and β forms of Ta_2C, take a surprising amount of "Ti_2C" into solid solution; this fact leads to the conclusion that the stability of a hypothetical "Ti_2C" is not exceptionally low. The peak of the "Ti_2C" phase on a plot of free energies of formation versus composition in the titanium-carbon system undoubtedly lies quite close to the tangent line connecting the maximum points of the titanium solid solution and the titanium

monocarbide. This supposition will be elucidated and expressed numerically using the data obtained from these phase equilibria investigations in the detailed thermodynamical treatment of this and other ternary systems given at a later date.

B. APPLICATIONS

The study of the titanium-tantalum-carbon-system has shown that there is a rather large area in the ternary system where the metal solid solution is in equilibrium with the monocarbide. Admittedly, the very high temperature applications of possible composite materials in the titanium metal-rich region are greatly limited by the appearance of liquid on the titanium side of the ternary at temperatures above 1650°C. However, with the proper selection, the maximum safe application temperature of composite bodies in this region would appear to be somewhat in excess of 1800°C. For rocket nozzle applications using a metal reinforcing principle, these temperatures are quite low. Another similar limiting factor is the lower melting points of the monocarbide solid solution itself, compared with similar alloys in other ternary carbide systems. In fact, the much lower melting point of the titanium-rich carbide solid solution, as well as the even lower melting titanium-rich monocarbide-graphite eutectic, would severely limit very high temperature applications of a titanium-rich carbide solution in contact with graphite even though there are no detrimental phase transformations in the monocarbide solid solution as there is in the sub-carbide.

Over the years, much use has been made of hard materials for cutting and grinding tools based on combinations such as WC-TiC-TaC;

the binding substances for these carbides have been in general cobalt, nickel, and iron. The working speeds of these tools has had to be limited to prevent the heat produced from deforming or even melting the tool itself.

It would seem possible to try to develop new cutting tools using the refractory metals and their alloys as a binder for the various carbide combinations. The necessary basic equilibria in this and other carbide systems exist; further investigations, both thermodynamical and experimental, would show how much of beneficial substitutional and additional materials would be tolerated by a given equilibrium before the equilibrium ceases to exist.

In the light of the views and the facts expressed above, it appears that the titanium-richer alloys of the Ti-Ta-C system show little promise for extremely high temperature applications. However, when and if the mechanical properties of such alloys are investigated, it may be found that many lower temperature applications indeed become feasible.

REFERENCES

1. E. Rudy, D.P. Harmon, and C.E. Brukl: AFML-TR-65-2, Part I, Vol. II. (May 1965)
2. E. Rudy, C.E. Brukl, and D.P. Harmon, AFML-TR-65-2, Part I, Vol V, May 1965
3. M. Hansen: Constitution of Binary Alloys, McGraw-Hill (1958) 383
4. I. Cadoff and J.P. Nielsen: Trans.AIME 197 (1953) 248-253
5. P. Ehrlich: Z. anorg. Chem. 259 (1949) 1-41
6. E. Friederich and L. Sittig: Z. anorg.Chem. 144 (1925) 171
7. C. Agte and K. Moers: Z. anorg.Chem. 198 (1931, 233
8. H. Nowotny and R. Kieffer: Z.Metallkunde 38 (1947) 257-265
9. J.T. Norton and A.L. Mowry: Trans.AIME 185 (1949), 133-136
10. E.K. Storms: Critical Review of Refractories, Part I (1962)
11. M.R. Nadler and C.P. Kempter: J.Phys.Chem. 64 (1925) 169
12. R.V. Sara and C.E. Lowell: WADD TDR-60-143, Part V, Oct. 1964
13. R. Kieffer and F. Benesovsky: Hartstoffe (Wein, Springer, 1963)
14. M.L. Pochon, C.R. McKinsey, R.A. Perkins, and W.P. Forgeng: Reactive Metals, Intersc. Publ. New York (1959), Vol. 2.
15. C.F. Zalabak: NASA-TN-D-761 (1961)
16. F. H. Ellinger: Trans. Am. Soc. Met. 31 (1943) 89
17. R. Lesser and G. Brauer: Z. Metallkunde 49 (1958) 622
18. W.G. Burgers and J.C.M. Basart: Z.anorg.allg.Chem.216 (1934)209
19. I.V. Smirnova and B.F. Ormont: Dokl.Akad.Nauk SSSR 96 (1954)557
20. A.L. Bowman: J. Phys. Chem. 65 (1961) 1956
21. E. Rudy, El. Rudy, and F. Benesovsky: Mh.Chem 93 (1962) 1176
22. M.G. Bowman: Metals for the Space Age (5th Plansee Seminar Proceedings, 1964, p 701)

References (continued)

23. B.W. Bonser: Ind. Eng. Chem. 42 (1950) 222

24. BMI: AF Tech. Report 6218, Part 2, June 1950, p.40.

25. D. Summers-Smith: J. Inst. Metals 81 (1952-53) 73

26. D.J. Maykuth, H.R. Ogden and R.I. Jaffee: Trans.AIME 197 (1953) 231

27. P. Duwez: Trans. ASM, 45 (1953) 934

28. M. Hansen: op. Cit. p. 1223.

29. H. Nowotny, R. Kieffer: Z. Metallkunde 38 (1947) 257

30. A.E. Koval'skii and J.S. Umanskii: Z.Fiz.Khim.SSSR 20 769

31. J.G. McMullin and J.T. Norton: J. Metals 5 (1953) 1205

32. J.T. Norton and A.L. Mowry: J. Metals 1, (1949), 133

33. E. Rudy, St.Windisch, and Y.A. Chang: AFML-TR-65-2, Part I, Vol I. Jan 1965

34. H.D. Heetderks, E. Rudy, and T. Eckert: AFML-TR-65-2, Part III, Vol. I. April 1965

35. Lit. Cit. 25 and 26 as reproduced in M. Hansen: Constitution of Binary Alloys, McGraw Hill (1958), 1223

36. Y.A. Chang: AFML-TR-65-2, Part IV, Vol I. May 1965

37. E. Rudy and H. Nowotny: Mh. Chem. 94, (1963) 507

38. E. Rudy: AFML-TR-65-2, Part II, Vol. I, May 1965

AEROJET-GENERAL CORPORATION
SACRAMENTO • CALIFORNIA

SACRAMENTO PLANT

2443:65-095:pjb
11 October, 1965

Subject: Report AFML-TR-65-2
Part II, Volume II
Ternary Phase Equilibria in Transition
Metal-Boron-Carbon-Silicon- Systems

To: Air Force Materials Laboratory
Research and Technology Division
Air Force Systems Command
Wright-Patterson Air Force Base, Ohio

Inclosure (1) is submitted in partial fulfillment of Contract AF 33(615)-1249.

AEROJET-GENERAL CORPORATION

RL Fulford

R. L. Fulford, Supervisor
Editorial Services
Technical Publications

Incl: (1) Copies 1 through 18, Report AFML-TR-65-2
Part II, Volume II

DOCUMENT CONTROL DATA - R&D

(Security classification of title, body of abstract and indexing annotation must be entered when the overall report is classified)

1. ORIGINATING ACTIVITY *(Corporate author)*
Materials Research Laboratory
Aerojet-General Corporation
Sacramento, California

2a. REPORT SECURITY CLASSIFICATION
Unclassified

2b. GROUP
N.A.

3. REPORT TITLE
Ternary Phase Equilibria in Transition Metal-Boron-Carbon-Silicon Systems
Part II. Ternary Systems, Volume II. Ti-Ta-C System

4. DESCRIPTIVE NOTES *(Type of report and inclusive dates)*

5. AUTHOR(S) *(Last name, first name, initial)*
C. E. Brukl
D. P. Harmon

6. REPORT DATE	7a. TOTAL NO. OF PAGES	7b. NO. OF REFS
September 1965	67	38

8a. CONTRACT OR GRANT NO.	9a. ORIGINATOR'S REPORT NUMBER(S)
AF 33(615)-1249	AFML-TR-65-2
b. PROJECT NO. 7350	Part II, Volume II
c. Task No. 735001	9b. OTHER REPORT NO(S) *(Any other numbers that may be assigned this report)*
d.	N.A.

10. AVAILABILITY/LIMITATION NOTICES
Qualified requesters may obtain copies of this report from DDC

11. SUPPLEMENTARY NOTES	12. SPONSORING MILITARY ACTIVITY
	AFML (MAMC) Wright-Patterson AFB, Ohio 45433

13. ABSTRACT

The ternary titanium-tantalum-carbon system was investigated using X-ray, DTA, melting point, and metallographic techniques on chemically analyzed alloys; a complete phase diagram for temperatures above 1500°C was established. The system contains a rather high melting, continuous monocarbide solid solution with a large carbon defect; a moderate titanium-tantalum exchange occurs in both the high and low temperature modifications of the subcarbide, Ta_2C. Two four-phase reaction planes are present in the metal-rich portion of the ternary diagram. The results of this investigation are described, discussed, and compared with another partial investigation of this system; possible applications are briefly mentioned.

DD FORM 1 JAN 64 1473

UNCLASSIFIED
Security Classification

Unclassified

Security Classification

14. KEY WORDS	LINK A		LINK B		LINK C	
	ROLE	WT	ROLE	WT	ROLE	WT
Ternary Phase Equilibria Carbide Systems High Temperature Titanium-Tantalum-Carbon						

INSTRUCTIONS

1. ORIGINATING ACTIVITY: Enter the name and address of the contractor, subcontractor, grantee, Department of Defense activity or other organization *(corporate author)* issuing the report.

2*a*. REPORT SECURITY CLASSIFICATION: Enter the overall security classification of the report. Indicate whether "Restricted Data" is included. Marking is to be in accordance with appropriate security regulations.

2*b*. GROUP: Automatic downgrading is specified in DoD Directive 5200.10 and Armed Forces Industrial Manual. Enter the group number. Also, when applicable, show that optional markings have been used for Group 3 and Group 4 as authorized.

3. REPORT TITLE: Enter the complete report title in all capital letters. Titles in all cases should be unclassified. If a meaningful title cannot be selected without classification, show title classification in all capitals in parenthesis immediately following the title.

4. DESCRIPTIVE NOTES: If appropriate, enter the type of report, e.g., interim, progress, summary, annual, or final. Give the inclusive dates when a specific reporting period is covered.

5. AUTHOR(S): Enter the name(s) of author(s) as shown on or in the report. Enter last name, first name, middle initial. If military, show rank and branch of service. The name of the principal author is an absolute minimum requirement.

6. REPORT DATE: Enter the date of the report as day, month, year; or month, year. If more than one date appears on the report, use date of publication.

7*a*. TOTAL NUMBER OF PAGES: The total page count should follow normal pagination procedures, i.e., enter the number of pages containing information.

7*b*. NUMBER OF REFERENCES: Enter the total number of references cited in the report.

8*a*. CONTRACT OR GRANT NUMBER: If appropriate, enter the applicable number of the contract or grant under which the report was written.

8*b*, 8*c*, & 8*d*. PROJECT NUMBER: Enter the appropriate military department identification, such as project number, subproject number, system numbers, task number, etc.

9*a*. ORIGINATOR'S REPORT NUMBER(S): Enter the official report number by which the document will be identified and controlled by the originating activity. This number must be unique to this report.

9*b*. OTHER REPORT NUMBER(S): If the report has been assigned any other report numbers *(either by the originator or by the sponsor)*, also enter this number(s).

10. AVAILABILITY/LIMITATION NOTICES: Enter any limitations on further dissemination of the report, other than those imposed by security classification, using standard statements such as:

(1) "Qualified requesters may obtain copies of this report from DDC."

(2) "Foreign announcement and dissemination of this report by DDC is not authorized."

(3) "U. S. Government agencies may obtain copies of this report directly from DDC. Other qualified DDC users shall request through

_____."

(4) "U. S. military agencies may obtain copies of this report directly from DDC. Other qualified users shall request through

_____."

(5) "All distribution of this report is controlled. Qualified DDC users shall request through

_____."

If the report has been furnished to the Office of Technical Services, Department of Commerce, for sale to the public, indicate this fact and enter the price, if known.

11. SUPPLEMENTARY NOTES: Use for additional explanatory notes.

12. SPONSORING MILITARY ACTIVITY: Enter the name of the departmental project office or laboratory sponsoring *(paying for)* the research and development. Include address.

13. ABSTRACT: Enter an abstract giving a brief and factual summary of the document indicative of the report, even though it may also appear elsewhere in the body of the technical report. If additional space is required, a continuation sheet shall be attached.

It is highly desirable that the abstract of classified reports be unclassified. Each paragraph of the abstract shall end with an indication of the military security classification of the information in the paragraph, represented as *(TS)*, *(S)*, *(C)*, *or (U)*.

There is no limitation on the length of the abstract. However, the suggested length is from 150 to 225 words.

14. KEY WORDS: Key words are technically meaningful terms or short phrases that characterize a report and may be used as index entries for cataloging the report. Key words must be selected so that no security classification is required. Identifiers, such as equipment model designation, trade name, military project code name, geographic location, may be used as key words but will be followed by an indication of technical context. The assignment of links, rules, and weights is optional.

UNCLASSIFIED

Security Classification